

Source parameters of the great Sumatran megathrust earthquakes of 1797 and 1833 inferred from coral microatolls

Danny Hilman Natawidjaja,^{1,2} Kerry Sieh,¹ Mohamed Chlieh,¹ John Galetzka,¹
Bambang W. Suwargadi,³ Hai Cheng,⁴ R. Lawrence Edwards,⁴
Jean-Philippe Avouac,¹ and Steven N. Ward⁵

Received 3 September 2005; revised 16 January 2006; accepted 17 March 2006; published 16 June 2006.

[1] Large uplifts and tilts occurred on the Sumatran outer arc islands between 0.5° and 3.3°S during great historical earthquakes in 1797 and 1833, as judged from relative sea level changes recorded by annually banded coral heads. Coral data for these two earthquakes are most complete along a 160-km length of the Mentawai islands between 3.2° and 2°S. Uplift there was as great as 0.8 m in 1797 and 2.8 m in 1833. Uplift in 1797 extended 370 km, between 3.2° and 0.5°S. The pattern and magnitude of uplift imply megathrust ruptures corresponding to moment magnitudes (M_w) in the range 8.5 to 8.7. The region of uplift in 1833 ranges from 2° to at least 3.2°S and, judging from historical reports of shaking and tsunamis, perhaps as far as 5°S. The patterns and magnitude of uplift and tilt in 1833 are similar to those experienced farther north, between 0.5° and 3°N, during the giant Nias-Simeulue megathrust earthquake of 2005; the outer arc islands rose as much as 3 m and tilted toward the mainland. Elastic dislocation forward modeling of the coral data yields megathrust ruptures with moment magnitudes ranging from 8.6 to 8.9. Sparse accounts at Padang, along the mainland west coast at latitude 1°S, imply tsunami runups of at least 5 m in 1797 and 3–4 m in 1833. Tsunamis simulated from the pattern of coral uplift are roughly consistent with these reports. The tsunami modeling further indicates that the Indian Ocean tsunamis of both 1797 and 1833, unlike that of 2004, were directed mainly south of the Indian subcontinent. Between about 0.7° and 2.1°S, the lack of vintage 1797 and 1833 coral heads in the intertidal zone demonstrates that interseismic submergence has now nearly equals coseismic emergence that accompanied those earthquakes. The interseismic strains accumulated along this reach of the megathrust have thus approached or exceeded the levels relieved in 1797 and 1833.

Citation: Natawidjaja, D. H., K. Sieh, M. Chlieh, J. Galetzka, B. W. Suwargadi, H. Cheng, R. L. Edwards, J.-P. Avouac, and S. N. Ward (2006), Source parameters of the great Sumatran megathrust earthquakes of 1797 and 1833 inferred from coral microatolls, *J. Geophys. Res.*, *111*, B06403, doi:10.1029/2005JB004025.

1. Introduction

1.1. Background

[2] Rupture of adjoining 1600- and 300-km sections of the Sunda megathrust in December 2004 and March 2005 generated two devastating great earthquakes and large tsunamis (Figure 1) [Subarya *et al.*, 2006; Briggs *et al.*, 2006]. These rapid fire failures of a long span of the

megathrust raise the question: Are unbroken sections to the north and south now close to failure? [Nalbant *et al.*, 2005; Sieh, 2005].

[3] One critical part of assessing whether or not they are close to failure is the investigation of the past behavior of each section of the megathrust. How have currently dormant sections failed in the past? Where have prior ruptures occurred, how large have they been, and how often and regularly do they recur?

[4] Most of the Sunda megathrust along the eastern margin of the Indian Ocean has generated large, destructive earthquakes in the past few centuries of historical record. North of the 2004 rupture, along the west coast of Myanmar, historical details are sparse, but Chhibber [1934] describes a large earthquake accompanied by uplift of coral reefs in 1762. In addition, strains now accumulating across the Indoburman ranges in western Myanmar can be ascribed in part to loading of an obliquely slipping Sunda megathrust [Vigny *et al.*, 2003].

¹Tectonics Observatory, California Institute of Technology, Pasadena, California, USA.

²Now at Research Center for Geotechnology, Indonesian Institute of Sciences, Bandung, Indonesia.

³Research Center for Geotechnology, Indonesian Institute of Sciences, Bandung, Indonesia.

⁴Department of Geology and Geophysics, University of Minnesota, Minneapolis, Minnesota, USA.

⁵Institute of Geophysics and Planetary Physics, University of California, Santa Cruz, California, USA.

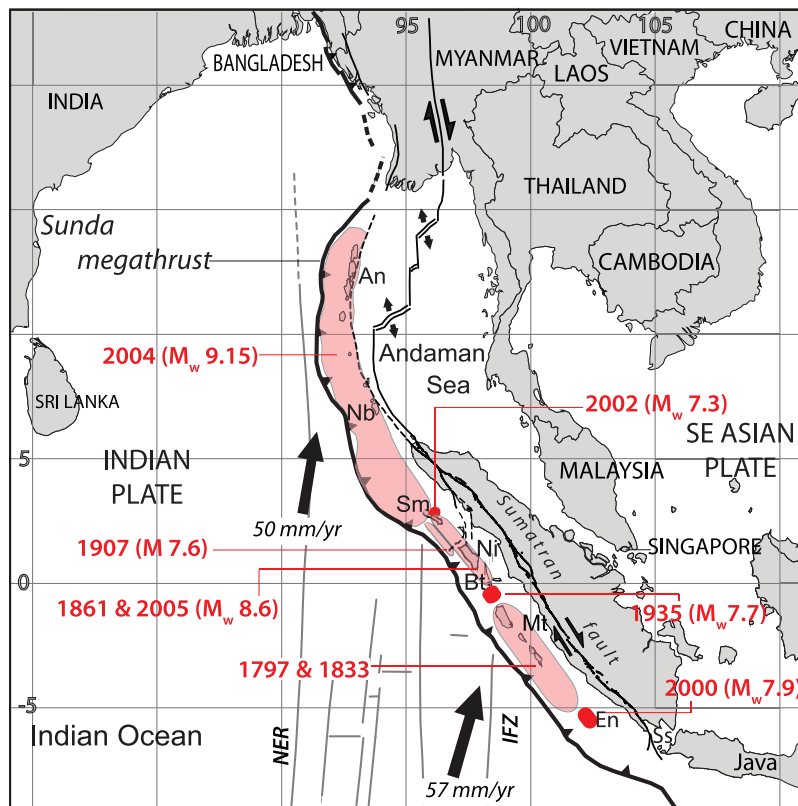


Figure 1. Tectonic and seismic setting of the Mentawai section of the Sunda megathrust. In the aftermath of the two giant Sumatran megathrust earthquakes of 2004 and 2005, the nature of past ruptures south of the equator is particularly worth investigating. The Mentawai islands (Mt) include all the islands within the ellipse labeled “1797&1833” and are the focus of this study. Ss, Sunda Strait; En, Enggano island; Bt, Batu islands; Ni, Nias island; Sm, Simeulue island; Nb, Nicobar islands; An, Andaman islands. NER and IFZ, Ninety-East Ridge and Investigator Fracture Zone. Intervening nearly north-south lines are other oceanic fracture zones, and intervening east-west lines are fossil spreading centers.

[5] The Sumatran section of the megathrust also has a history of destructive large earthquakes (summarized by *Newcomb and McCann* [1987]), and geodetic measurements show that strain accumulates there in a manner consistent with most of the megathrust being locked [*Prawirodirdjo et al.*, 1997; *Chlieh et al.*, 2005]. Although the 2004 Aceh-Andaman earthquake is without known precedent, a large earthquake with a magnitude and source area similar to the 2005 Nias-Simeulue earthquake occurred in 1861 (Figure 1) [*Newcomb and McCann*, 1987; *Wichmann*, 1918]. A smaller rupture in the region in 1907 produced a higher and more destructive tsunami on the western coast of Simeulue than occurred in 2004 or 2005 [*Newcomb and McCann*, 1987; *Briggs et al.*, 2006]. This may mean that large slips occurred on the shallow section of the megathrust between the island and the trench. Near the equator, a narrow, 70-km-long section of the megathrust produced an M_w 7.7 earthquake in 1935 [*Natawidjaja et al.*, 2004; *Rivera et al.*, 2002].

[6] The largest historical Sumatran earthquake originated south of the equator in 1833 [*Newcomb and McCann*, 1987]. Reports of severest shaking are from Bengkulu to Pariaman and at sea near the Pagai islands (Figure 2 and Appendix A). Tsunamis along that same stretch of the coast were destructive, especially at Indrapura and Bengkulu, and

subsequent minor activity occurred at three nearby Sumatran volcanoes. The tsunami height at the coast of Padang is reported to have been 3–4 m. The extent of severest effects coupled with seismotectonic considerations led *Newcomb and McCann* [1987] to conclude that the rupture extended about 550 km, from near Enggano island in the south to the Batu islands in the north. On the basis of this extent, they calculated the size of the earthquake to be between M_w 8.7 and 8.8. Studies of uplifted coral on the fringing reefs of Sipora, North Pagai, and South Pagai islands show that at least a 140-km length of the megathrust beneath these islands participated in the 1833 rupture [*Zachariassen et al.*, 1999]. The elastic dislocation model that fit their coral uplift data best had 13 m of slip on the underlying megathrust. This corresponds to an M_w 8.8, if slip occurred only under these islands, but an M_w 9.2 if rupture extended the full 550 km proposed by *Newcomb and McCann* [1987].

[7] A previous large earthquake, in 1797, was accompanied by a destructive tsunami at Padang [*Newcomb and McCann*, 1987] (Appendix A). The only reports of shaking and tsunami damage are from Padang and nearby, which suggests that Bengkulu, which was also a bustling settlement at the time, was not greatly affected. The shaking is

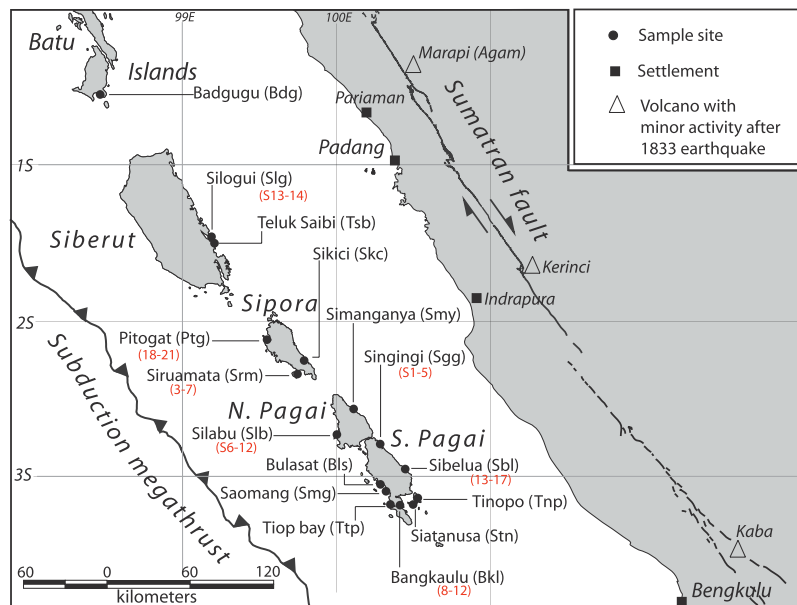


Figure 2. Map of sampled sites on the Sumatran outer arc islands that have evidence for emergence in 1797 and/or 1833. Data from three sites (Tiop bay, Siatanusa, and Tinopo) are from *Zachariassen et al.* [1999]. Siberut, Sipora, North Pagai, and South Pagai are the largest of the Mentawai islands. Numbers in parentheses refer to figures in the text and in the auxiliary material that illustrate data from the sites.

reported to have been the strongest in living memory at Padang, and the tsunami flow depth there was likely at least 5 m.

[8] In this paper we use coral stratigraphy to build upon the investigations of *Zachariassen et al.* [1999] to constrain further the source parameters of the great 1833 earthquake. In the process, we also produce evidence for the source of the 1797 earthquake and show that it was larger than previously thought [*Newcomb and McCann, 1987*].

1.2. Coral Microatolls as Recorders of Paleogeodetic Vertical Deformation

[9] Coral “microatolls” provide an exceptional opportunity to understand tectonic strain accumulation and relief. They are so named [*Krempf, 1927; Scoffin and Stoddart, 1978*] because those with raised rims and low centers resemble the celebrated island atolls that form on slowly submerging tropical oceanic crust [*Darwin, 1842*]. Several species of the genera *Porites* and *Goniastrea* produce this form when they grow near lowest low tide levels on submerging coastlines.

[10] Microatoll morphologies form because the upward growth of corals heads is limited by lowest tide levels, above which exposure causes death. This uppermost limit to coral growth is called the HLS, an acronym for the highest level of survival [*Taylor et al., 1987*]. Fluctuations in HLS are imprinted on the morphology and stratigraphy of microatolls that have grown up to the level of lowest low tide, as described and illustrated in Appendix B and at <http://es.ucsc.edu/~ward/Srm00A1.mov>.

[11] A year’s coral growth typically produces a pair of bands, one dark and one light, that reflect seasonal variations in the density of the coral skeleton caused by seasonal variations in sea temperature, rainfall, and other factors [*Knutson et al., 1972; Scoffin and Stoddart, 1978; Taylor*

et al., 1987; Zachariassen et al., 1999]. The light, lower-density band grows during the rainy season (September to March), and the dark, higher-density band forms during the dry season (April to August) [*Zachariassen, 1998*]. The annual band is similar to a tree ring in that it provides a yearly record of growth. Taken together a series of annual bands thus provides a time series for constructing a sea level history. The annual bands are sometimes visible to the naked eye, but are more pronounced in X radiographs of thin slabs that have been cut parallel to the direction of coral growth.

[12] As stable, long-lived, natural recorders of both slow and abrupt change in sea level relative to their substrate, with sensitivities of about 20 mm, living microatolls are natural “paleogeodetic” gauges that enable examination of relative sea level time series in places and over times not covered by instrumental recordings [*Zachariassen et al., 2000; Sieh et al., 1999*]. Moreover, advances in U-Th disequilibrium geochronology since the mid-1980s allow dating of annual growth bands in fossil microatolls with uncertainties of only a few years to a few decades, so rates and dates of vertical motions can be constrained tightly [*Edwards et al., 1988; Taylor et al., 1990; Zachariassen et al., 1999; Shen et al., 2002; Cobb et al., 2003; Natawidjaja et al., 2004*]. In the case of western Sumatra, one also has historical evidence that allows association of specific events in a dated coral microatoll to historical earthquakes.

[13] Two attributes of western Sumatra make its populations of microatolls particularly well suited for studying the cyclic accumulation and relief of tectonic strains. First, the Sumatran part of the Sunda subduction zone is one of only a few subduction margins with an abundance of coastline above the locked parts of the subduction megathrust. These coastlines range from 70 to 150 km landward of the trench axis and about from about 20 to 35 km above the mega-

thrust. Second, the region's late Holocene vertical motions are predominantly elastic deformations associated with the cyclic accumulation and relief of strain. Throughout the region, the presence of mid-Holocene microatolls near sea level shows that permanent tectonic deformations have been comparatively slight over the past several thousand years [Zachariassen, 1998].

2. Methods

2.1. Mapping, Collecting, Sample Preparation, and Analysis

[14] At sites where we wanted to establish HLS time series, we mapped the intertidal reef, documented the height, shape and dimensions of many of the coral heads, and collected slab samples from heads that were representative of the overall population. Use of a handheld GPS receiver with an accuracy of 10 m or better and an electronic total station with accuracy of a few millimeters provided control for both coarse and detailed mapping. A hydraulic chainsaw designed for underwater use enabled collection of vertically oriented ~150-mm-wide slabs from the microatoll. We surveyed the elevations of the upper surfaces of the sampled microatolls prior to cutting and removal of the slabs, to enable recovery of a vertical datum and its relationship to sea level and other samples after removal of the slab.

[15] Usually we were able to sample from sites where our slabs represented a larger population of coral heads displaying a similar history. We avoided collecting from microatolls whose HLS history might not reflect open ocean sea level [Scoffin and Stoddart, 1978]. Whenever possible we collected samples from microatolls that were unaffected by local tilting or subsidence. Such disturbances are easily recognizable, either by visual inspection in the field or by anomalous elevations relative to other heads at the site.

2.2. Preparation and Analysis of the Samples

[16] Subsequent to collection, we used a large circular saw to cut a thinner section, typically about 10 mm thick, from each slab. X radiographs of these sections reveal details of growth that are otherwise invisible to the eye. We then used scans of the X radiographs to produce stratigraphic sections that depict the annual banding of the microatoll.

2.3. Radiometric Dating of the Microatolls

[17] After collection in the field but before cutting into thin slabs, we used a handheld diamond-impregnated hole drill to remove 5-mm-diameter cores for U-Th dating. The dating was performed at the University of Minnesota. For each analysis, we selected and dissolved samples weighing about 350 mg. Procedures for analysis were modifications of those originally described by Edwards et al. [1987]. Cheng et al. [2000] describes standards and spikes, and Shen et al. [2002] describe mass spectrometric analysis. Each dissolved sample was spiked with a mix of ^{233}U , ^{236}U , and ^{229}Th . Purified uranium and thorium fractions were separated using iron hydroxide precipitation and anion exchange techniques. These fractions were dissolved in dilute nitric acid and their isotopic compositions determined by aspirating solutions through a desolvation nebulizer

(MCN 6000 from Cetac Technologies) and measuring ion beam ratios on a magnetic sector inductively coupled plasma mass spectrometer (Thermo-Finnigan Element) operated in peak-jumping and pulse-counting modes using a guard electrode. Tables 1 and S1 in the auxiliary material display the results of these measurements.¹

3. Tectonics and Seismic History of the Active Sumatran Plate Boundary

[18] Convergence of the Australian and Indian plates toward southeast Asia is highly oblique at the latitudes of Sumatra (Figure 1). The obliquity is almost completely partitioned into a frontal dip-slip component, accommodated by slip on the subduction megathrust and a right-lateral strike-slip component, accommodated by the Sumatran fault [Fitch, 1972; Katili and Hehuwat, 1967; McCaffrey, 1991].

[19] Five great or giant earthquakes dominate strain relief along the subduction megathrust during the period of historical record: In addition to the Aceh-Andaman M_w 9.15 earthquake of 2004 [Subarya et al., 2006] and the Nias-Simeulue M_w 8.6 earthquake of 2005 [Briggs et al., 2006], $M_w \sim 9$ and $M_w \sim 8.5$ earthquakes occurred in 1833 and in 1861, respectively [Newcomb and McCann, 1987](Figure 1). In this paper, we show that an earthquake in 1797 also belongs in this group of great earthquakes.

[20] Smaller large megathrust earthquakes have occurred at the termini of these great and giant earthquakes, as well (Figure 1). An M_w 7.3 event [DeShon et al., 2005] occurred at the join between the 2004 and 2005 ruptures in 2002. A short length of the megathrust near the equator produced an M_w 7.7 earthquake in 1935. Microatoll records show that the earthquake resulted from about 2.3 m of slip on a 35-km-wide, 70-km-long patch of the megathrust between the equator and about 0.7°S [Rivera et al., 2002; Natawidjaja et al., 2004]. Microatolls also show that this has been the largest rapid slippage on this part of the megathrust over the past 250 years and that most slip on this patch has been occurring aseismically for at least the past half century. Thus this section of the megathrust separates the sections to the south and north that generate great and giant earthquakes, perhaps not unlike the separation of locked sections of the San Andreas fault by its 170-km-long, central creeping reach [Allen, 1968].

[21] The second important smaller earthquake is an M_w 7.9 event that occurred near Enganno island in 2000, near what was inferred from historical accounts of shaking and tsunamis and a concentration of background seismicity [Newcomb and McCann, 1987] to be the end of the 1833 rupture. Abercrombie et al. [2003] found the 2000 earthquake to be complex. It involved sequential rupture of a left-lateral north striking strike-slip fault within the down-going oceanic slab and then rupture of the megathrust. The strike-slip structure may be one of a set of similar structures between the Investigator fracture zone and Ninety-East ridge offshore Sumatra [Deplus et al., 1998] that accommodate relative motions between the Australian and Indian plates (Figure 1).

¹Auxiliary material is available at <ftp://ftp.agu.org/apend/jb/2005jb004025>.

Table 1. The ^{230}Th Ages of Sumatran Microatolls Reported in This Paper^a

Sample	^{238}U , ppb	^{232}Th , ppt	$\delta^{234}\text{U}$ (Measured) ^b	$^{230}\text{Th}/^{238}\text{U}$ (Activity)	^{230}Th Age, years		Calendar Year ^c	$\delta^{234}\text{U}_{\text{Initial}}$ (Corrected) ^d
					Uncorrected	Corrected		
<i>Bangkaulu (Bkl)</i>								
Bkl03A1-1b	2205 ± 3	2030 ± 9	145.1 ± 1.8	0.00243 ± 0.00004	233 ± 4	198 ± 35	1807 ± 35	145.2 ± 1.8
Bkl03A1-2b	2230 ± 2	2903 ± 8	147.2 ± 1.3	0.00284 ± 0.00004	272 ± 4	223 ± 49	1782 ± 49	147.2 ± 1.3
Bkl03A3-1a (I)	2142 ± 3	247 ± 8	144.4 ± 2.3	0.00015 ± 0.00004	16 ± 4	11 ± 6	1994 ± 6	145.5 ± 1.4
Bkl03A3-1a (II)	2147 ± 5	176 ± 8	146.8 ± 3.1	0.00022 ± 0.00004	22 ± 4	19 ± 5	1986 ± 5	146.8 ± 3.1
Bkl03A3-2a	2354 ± 5	306 ± 6	148.5 ± 2.2	0.00053 ± 0.00004	51 ± 3	46 ± 6	1959 ± 6	148.5 ± 2.2
Bkl03A2-1b	2087 ± 2	243 ± 6	145.4 ± 1.4	0.00219 ± 0.00003	210 ± 3	205 ± 5	1800 ± 5	145.5 ± 1.4
<i>Sibelua (Sbl)</i>								
Sbl02A1-1a	2098 ± 2	831 ± 5	145.3 ± 1.2	0.00215 ± 0.00003	207 ± 3	193 ± 15	1812 ± 15	145.4 ± 1.2
Sbl02A1-2b	2124 ± 2	1995 ± 5	147.0 ± 1.2	0.00294 ± 0.00003	282 ± 3	247 ± 35	1758 ± 35	147.1 ± 1.2
Sbl02A1-4a	2103 ± 3	1741 ± 7	147.1 ± 1.9	0.00360 ± 0.00004	344 ± 4	313 ± 31	1692 ± 31	147.2 ± 1.9
Sbl02A2-2a (I)	2203 ± 2	1566 ± 8	145.0 ± 1.6	0.00086 ± 0.00006	84 ± 6	57 ± 27	1948 ± 27	145.1 ± 1.6
Sbl02A2-2a (II)	2180 ± 2	1664 ± 8	145.4 ± 1.2	0.00094 ± 0.00003	91 ± 3	63 ± 29	1942 ± 29	145.4 ± 1.2
<i>Pitogat (Ptg)</i>								
Ptg00A2 1a	2363 ± 4	1466 ± 12	145.3 ± 2.1	0.00258 ± 0.00007	251 ± 6	228 ± 24	1777 ± 24	145.4 ± 2.1
Ptg00A2 3b	2368 ± 3	628 ± 12	148.3 ± 1.5	0.00275 ± 0.00004	267 ± 4	260 ± 5	1745 ± 5	148.4 ± 1.5
PTG00A1 2a	2404 ± 4	4799 ± 18	146.1 ± 1.6	0.00112 ± 0.00004	110 ± 4	36 ± 75	1969 ± 75	146.1 ± 1.6
PTG00A1 2b	2675 ± 5	2117 ± 14	144.9 ± 2.0	0.00083 ± 0.00003	83 ± 3	53 ± 30	1952 ± 30	144.9 ± 2.0

^aSamples have been dated by the U-Th disequilibrium method [Edwards *et al.*, 1987], modified as described by Cheng *et al.* [2000], at the University of Minnesota. The unit ppt refers to parts per trillion by mass. Ages and ^{234}U values are calculated using decay constants from Cheng *et al.* [2000]. Uncorrected ^{230}Th ages are calculated assuming no initial ^{230}Th . Corrected ^{230}Th ages are our best estimate of the true age on the basis of the samples' isotopic composition. The ages are corrected for initial ^{230}Th assuming an initial atomic $^{230}\text{Th}/^{232}\text{Th}$ ratio of $(6.5 \pm 6.5) \times 10^{-6}$. This value is specific to corals from this area [Zachariassen *et al.*, 1999]. The initial ^{234}U value is calculated from the measured ^{234}U value using the corrected ^{230}Th age. U-Th data for samples from Si94A6 are from Zachariassen *et al.* [1999]. Here $\lambda_{230} = 9.1577 \times 10^{-6} \text{ yr}^{-1}$, $\lambda_{234} = 2.8263 \times 10^{-6} \text{ yr}^{-1}$, and $\lambda_{238} = 1.55125 \times 10^{-10} \text{ yr}^{-1}$.

^bHere $\delta^{234}\text{U} = ([^{234}\text{U}/^{238}\text{U}]_{\text{activity}} - 1)1000$.

^cYears on the left side are determined by subtracting the corrected ^{230}Th age from the date of analysis.

^dHere $\delta^{234}\text{U}_{\text{initial}}$ was calculated based on ^{230}Th age (T), i.e., $\delta^{234}\text{U}_{\text{initial}} = \delta^{234}\text{U}_{\text{measured}} (e^{\lambda_{234}T})$.

[22] Recent deformation of western Sumatra has been documented by campaign-style GPS measurements made between 1989 and 2000 [Prawirodirdjo *et al.*, 1999; Bock *et al.*, 2003]. These data show that the large islands south of the equator, in the area of the 1833 source rupture, are moving in the direction of the relative plate motion vector. These motions indicate that the subjacent subduction interface is fully locked [Prawirodirdjo *et al.*, 1997]. By contrast, the GPS stations on the islands around the equator, above the 1935 source, experience lesser motions that are more nearly parallel to the trench (unpublished data, SuGAR network). These surface movements indicate significant aseismic slip on the interface. This part of the subduction interface is within a tectonic domain where the overriding plate is structurally more complex than it is farther south [Sieh and Natawidjaja, 2000].

[23] Zachariassen *et al.* [1999] report U-Th ages that cluster around 1833 from microatolls at 15 sites around the Mentawai archipelago. All but three of these sites are on the coast of southern South Pagai (Figure 2). At most sites, they collected small samples with rock hammer and chisel. However, at six locations, Silabu, Siruamata, Saomang, Tiop Bay, Siatanusa, and Tinopo islands, they cut vertical slabs of the 1833 heads and were able to analyze the history of vertical deformation leading up to emergence in 1833. We have revisited the Silabu, Siruamata and Saomang sites and offer updates to their interpretations below. Although we did not collect new material from their Tiop bay site, we have revised their analyses in the light of what we have found at other sites.

[24] The basic observation of the earlier microatoll work is that southern South Pagai island rose and tilted toward the

mainland in 1833. Zachariassen *et al.* [1999] reported uplift of about 2 m on west coast and about 1 m on east coast. They estimated the 1833 coseismic step as we have done, by extrapolating the rate of submergence of a modern microatoll to 1833 to get the immediately post-1833 HLS and then subtracting that elevation from the elevation of the immediately pre-1833 HLS. Only at two of their sites, however, did they collect slabs from both modern and fossil microatolls, so they had to estimate modern rates from other sites.

[25] The emergence values they document implied about 13 m of slip on the megathrust beneath southern South Pagai. Assuming similar slip under Sipora and North Pagai, they calculated the size of the 1833 earthquake to be $M_w 8.8$. They extrapolated to an $M_w 9.2$ by assuming that the rupture extended with the same parameters from the equator to 5.5°S, the rupture length Newcomb and McCann [1987] had inferred from historical reports of shaking and tsunamis.

4. Results From Individual Sites

[26] The data upon which this paper is based come from 14 sites, 13 from the coasts of the four major Mentawai islands (Siberut, Sipora, and North and South Pagai) and one in the Batu islands (Figure 2). Three sites studied previously [Zachariassen *et al.*, 1999] were not visited by us. We visited the remaining 11 in 1999, 2000, 2002, and 2003. This report contains the detailed record of seven of these sites: four in the main text, as examples of the nature of the data, and three in the auxiliary material (Text S2). Details of the other four sites will appear in future publications that describe evidence for repeated large mega-

Table 2. Locations of All Microatolls Used in This Study, Determined With Handheld GPS Receivers^a

Site	Sample	Longitude	Latitude
Badgugu, Tanamasa	Bdg00A1	98.46394	-0.53928
Silogui, Siberut	Slg02A1	99.03441	-1.22577
Teluk Saibi	Tsa00A1	99.07342	-1.26871
Pitogat, Sipora	Ptg02A2	99.53684	-2.13201
Pitogat, Sipora	Ptg02A1	99.53567	-2.13171
Siruamata, Sipora	Si94A6	99.74520	-2.36946
Siruamata, Sipora	Srm00A1	99.74060	-2.37033
Sikici-Site B, Sipora	Skc03B3	99.78369	-2.28726
Sikici-Site A, Sipora	Skc00A1	99.80205	-2.28943
Silabusabeu, North Pagai	Slb00A1	99.99514	-2.75206
Silabusabeu, North Pagai	Slb00A2	99.99546	-2.75128
Silabusabeu, North Pagai	Slb00A3	99.99546	-2.75128
Silabusabeu, North Pagai	Slb00A4	99.99485	-2.75098
Silabusabeu, North Pagai	Np94A8	99.99519	-2.75162
Simanganya-Site C, North Pagai	Smy03C3	100.11115	-2.60447
Simanganya-Site A, North Pagai	Np00A1	100.10150	-2.59419
Singingi, South Pagai	Sgg03A1	100.28340	-2.82576
Singingi, South Pagai	Sgg03A2	100.28309	-2.82615
Singingi, South Pagai	Sgg03A3	100.28281	-2.82588
Singingi, South Pagai	Sgg03A5	100.28327	-2.82456
Sibelua, South Pagai	Sbl02A1	100.46258	-3.03911
Sibelua, South Pagai	Sbl02A2	100.46251	-3.03799
Bulasat, South Pagai	Bls02A5	100.31110	-3.12747
Saomang, South Pagai	Smg02A2	100.31078	-3.12898
Bangkaulu, South Pagai	Bkl03A1	100.44632	-3.28526
Bangkaulu, South Pagai	Bkl03A2	100.44627	-3.28504
Bangkaulu, South Pagai	Bkl03A3	100.44658	-3.28521
Tinopo, South Pagai	P96K2	100.50499	-3.16275
Siatanusa, South Pagai	P96J3	100.48669	-3.21589
Teluk Tiop, South Pagai	P96H1	100.33245	-3.21055

^aWe have found the locations are repeatable from year to year to within about 10 m or less.

thrust ruptures beneath the Mentawai islands and for long-term aseismic behavior beneath the Batu islands.

[27] At each of the 11 sites, we collected slabs from both fossil and modern microatoll heads. These give constraints on coseismic uplift in 1797 and 1833 and on the rates of vertical deformation for three periods, the decades prior to 1797, the 27 years between 1797 and 1833, and the latter half of the 20th century. Tables 1 and S1 list the U-Th analyses that constrain the dates of growth of the slabs discussed in detail in this paper. Table 2 lists the latitude and longitude of each sampled microatoll.

4.1. Siruamata Site (Srm)

[28] This locality provides a representative example of the recent paleoseismic record along the southwestern coasts of the Mentawai islands. It lies on the east coast of Siruamata islet, a few kilometers off the southwestern coast of Sipora island (Figure 2). Zachariassen *et al.* [1999] estimated emergence of about 0.7 m during a historically unreported event in about 1810, followed by emergence of about 0.9 m in 1833. Our interpretation differs from theirs because we have new evidence that places the 0.7-m emergence in 1797 and because we have sampled a modern microatoll at the site to constrain better the emergence in 1833.

[29] The sampled living and fossil microatolls are separated by about half a kilometer. The living head sits on the edge of a mangrove swamp; the fossil microatolls sampled by Zachariassen *et al.* [1999] populate an intertidal reef platform that extends out from a narrow beach (Figures 3 and 4).

4.1.1. Analysis of a Modern Head

[30] The sample taken from the large modern *Porites* microatoll, Srm00A1, contains a 50-year record of submergence (Figure 5). In that record, the El Niño years of 1962, 1983, 1994, and 1997 [Saji *et al.*, 1999], with their characteristically exceptional low tides, manifest themselves in the record as HLS unconformities. Otherwise the record is one of uninhibited upward growth. The average rate of submergence of the reef during the 5 decades of record is about 8 mm/yr, just a few mm/yr under the maximum rate at which an unimpeded coral can grow upward [Natawidjaja *et al.*, 2004]. An animated simulation of the growth of this microatoll in response to sea level changes is available at <http://es.ucsc.edu/~ward/Srm00A1.mov>.

4.1.2. Reanalysis of Fossil Head Si94A6

[31] Fossil microatoll Si96A6 is representative of a number of microatolls discovered by Zachariassen *et al.* [1999]. It has a central flat surrounded by a younger and higher outer raised rim, and the base of that outer raised rim is surrounded by a disk of still younger growth (Figure 6). The 0.7-m drop from top of the high to the top of the low outer rim represents an emergence of the coral. The abrupt thinning of annual bands 23 bands in from the perimeter of the slab is coincident with the time of the emergence, when the microatoll base suddenly became exposed to low-tide water depths of only a couple tens of centimeters. It may be that the thinner bands indicate that survival was more difficult in the hotter water that would have formed during low tides after uplift. Erosion of several centimeters of coral from the lower flank of the microatoll is clear in the cross section. This commonly occurs on the flanks of microatolls that have been lifted into the intertidal zone [Natawidjaja *et al.*, 2004]. An animated simulation of the



Figure 3. Oblique aerial photograph of the Siruamata site. Fossil microatoll Si94A6 is underwater in the lower left corner of the image. The sampled living microatoll Srm00A1 is in front of the sparse mangroves in the center right. View is approximately southward. Naming convention for coral heads and samples is as follows: First two or three letters are abbreviations for the site or island name; next two numbers refer to the year the coral was studied or sampled; next letter indicates the subsite on the island; last number is a specific number for the coral head. Hence Srm00A1 denotes the first head measured or sampled (1) at the first site studied (A) on Siruamata island (Srm) in the year 2000 (00).

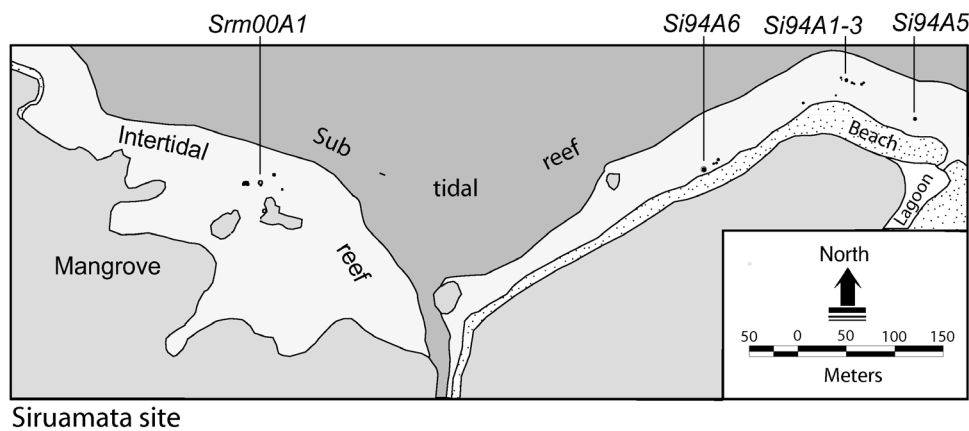


Figure 4. Map of the Siruamata site showing the location of the slabbed modern microatoll (Srm00A1) and fossil microatolls described by Zachariassen *et al.* [1999].

growth of this microatoll in response to sea level changes is available at <http://es.ucsc.edu/~ward/S94A6.mov>.

[32] Annual banding of Si94A6 is exceptionally clear, so relative ages of the annual bands are certain within only a year or two. Two U-Th dates constrain the date of the 0.7-m emergence event to near the end of the 18th century. U-Th analyses permit Zachariassen *et al.*'s [1999] interpretation that the outermost ring is the 1833 annual band. However, this interpretation means that the 0.7-m emergence would have occurred within a few years of 1810, a period during which the historical record is devoid of large earthquakes.

[33] It is also possible to assign the 0.7-m emergence to 1797, the year of a large, tsunamigenic earthquake in the historical record [Newcomb and McCann, 1987] (Appendix A). The U-Th ages of Zachariassen *et al.* [1999] permit this interpretation. Additional support for a 1797 date of emergence comes from the temporal pattern of $\delta^{13}\text{C}$ values in the last 2 decades of growth. In search of an isotopic signal reflecting a sudden change in light conditions associated with uplift in this well-banded slab, our colleague, M. Gagan, conducted a detailed examination of $\delta^{13}\text{C}$ variations through the outermost bands of the slab [Gagan *et al.*, 2000]. The clear annual signal in the record likely reflects a pronounced difference in corallite metabolism between the rainy/cloudy and dry/sunny seasons. This annual pattern breaks down once in the time series, in the fifth youngest wholly preserved band. If, as inferred by Gagan *et al.*, this band represents the “year without a summer” following the eruption of Tambora, east of Java, in April 1815, 1797 is the date of the last thick ring that grew prior to the 0.7-m emergence. This date of emergence is only a couple years older than the date derived from the two U-Th analyses shown in Figure 6. Counting out from the sampled rings to the youngest thick ring yields estimates of A.D. 1801 ± 5 and 1807 ± 7 . The weighted average of these dates is A.D. 1803 ± 4 .

[34] Although this interpretation is consistent with the U-Th dates, it would mean that the microatoll died in 1820 rather than in 1833. Claiming that the death of the head was from nontectonic causes in 1820 is not strictly ad hoc, since the extraordinary thinness of the annual bands after the 0.7-m emergence attests to the fact that the head was stressed in its final decades [Zachariassen *et al.*, 1999].

4.1.3. Emergence in 1797 and 1833

[35] Combination of the fossil and modern HLS histories allows a more precise estimate of the 1833 coseismic step. Figure 7 shows that the elevation of the pre-1833 HLS was about 0.1 m below modern HLS in 2000. A linear extrapolation of the modern HLS back to 1833, using the rate of submergence determined from the modern microatoll, yields an HLS elevation just after the 1833 event about 1.4 m below the HLS in 2000. The difference between preevent and postevent HLS, about 1.2 m, is an estimate of uplift in 1833.

[36] Linear extrapolation of the modern HLS back to 1833 may yield an underestimate of the actual coseismic uplift in 1833, since large postseismic transients are common following large earthquakes [Sawai *et al.*, 2004; Melbourne *et al.*, 2002]. For example, above the Sumatran megathrust a postseismic transient is evident in some of the microatoll records of the $M_w 7.7$ rupture of 1935, a few hundred kilometers northwest of Siruamata [Natawidjaja *et al.*, 2004]. Postseismic subsidence of some coseismically uplifted sites continues even today at a higher rate than was occurring in the decades prior to the 1935 earthquake. Continuous GPS records above the 2005 rupture of the megathrust also record postseismic transients. At Lahewa, where coseismic uplift was nearly 3 m, subsidence of 150 mm occurred in just the first 4 months following the earthquake [Hsu *et al.*, 2005]. These examples show that we could be underestimating significantly the 1833 coseismic step, not only at Siruamata but at other sites as well. However, we use a linear extrapolation of the modern rate back to 1833 because we have no direct knowledge of postseismic transients.

[37] Furthermore, the effect of postseismic subsidence would be offset to some degree by the modern global rise in sea level. Whereas inclusion of postseismic subsidence would increase our estimate of coseismic uplift, correction of the modern subsidence rate by the amount of modern global sea level rise would reduce it. Since at least 1870, global sea level has been rising [Church and White, 2006]. This correction would be about 195 mm for the period from 1870 to 2000 and, by extrapolation, about 200 mm for the entire period between our sample collection dates and the 1833 earthquake. We have not

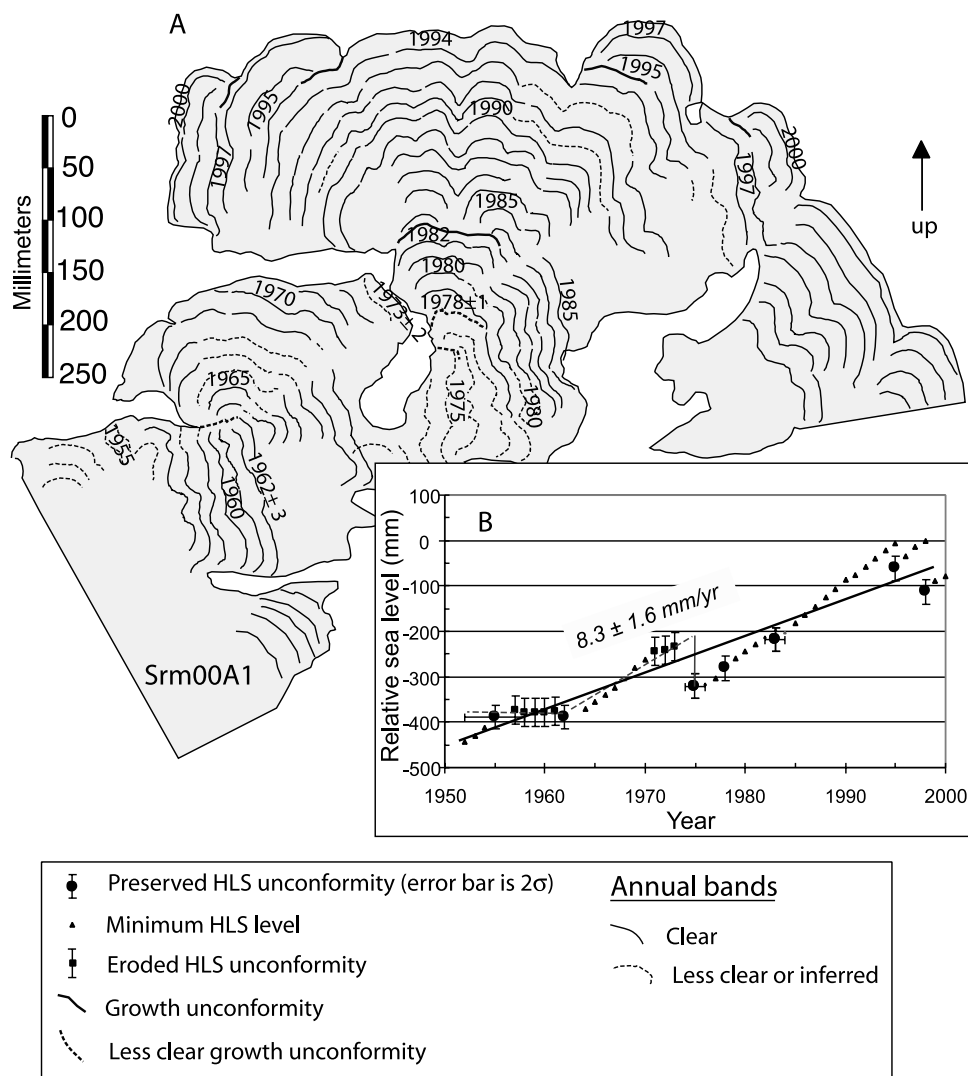


Figure 5. Modern history of sea level change revealed in microatoll Srm00A1 at Siruamata. (a) Drawing of the vertical face of a radial cut through the coral microatoll. Concentric annual growth bands indicate unimpeded lateral and vertical growth, when corallites are growing below the level of lowest low tide, which is just a few centimeters below the highest level at which they can survive (HLS). Heavy lines are unimpeded growth, commonly formed when upward growth is unimpeded by aerial exposure during lowest low tides but also caused by tectonic emergence above lowest low tides. Dates of formation of the annual bands were determined by counting inward from the outer perimeter, which was living when the slab was collected, in mid-2000. Date uncertainties reflect ambiguities in that count. In this microatoll, progressively higher HLS unimpeded growths in about 1962, 1974, 1983, 1994, and 1997 indicate rapid submergence since 1962. (b) Graph of HLS history derived from the microatoll cross section shows an average rate of submergence of about 8 mm/yr for the past 5 decades. Circles denote HLS unimpeded growth. Squares indicate eroded HLS unimpeded growth. Small triangles show highest level of coral growth for years in which the entire coral head was growing below HLS. These are lower bounds on HLS.

made this correction in any of our reconstructions of the 1833 coseismic step.

4.2. Bangkaulu Site (Bkl)

[38] The Bangkaulu site is representative of three sites on southern South Pagai island that show little to no emergence during the 1797 event but clear evidence for uplift in 1833. The site is on the east coast of a long narrow peninsula that extends South Pagai southeastward (Figure 2). Bangkaulu

village lies about 2 km to the northwest. The site consists of a small beach berm and intertidal reef with sparse stands of mangrove nearshore (Figure 8). Many well-preserved small fossil *Goniastrea* microatolls lie within and close to the beach face and mangrove thicket (Figure 9). A few larger *Porites* microatolls exist farther from shore, and a band of their living equivalents lies tens of meters still farther from shore. The elevation difference of about 0.1 m between the tops of the fossil *Goniastrea* and *Porites*

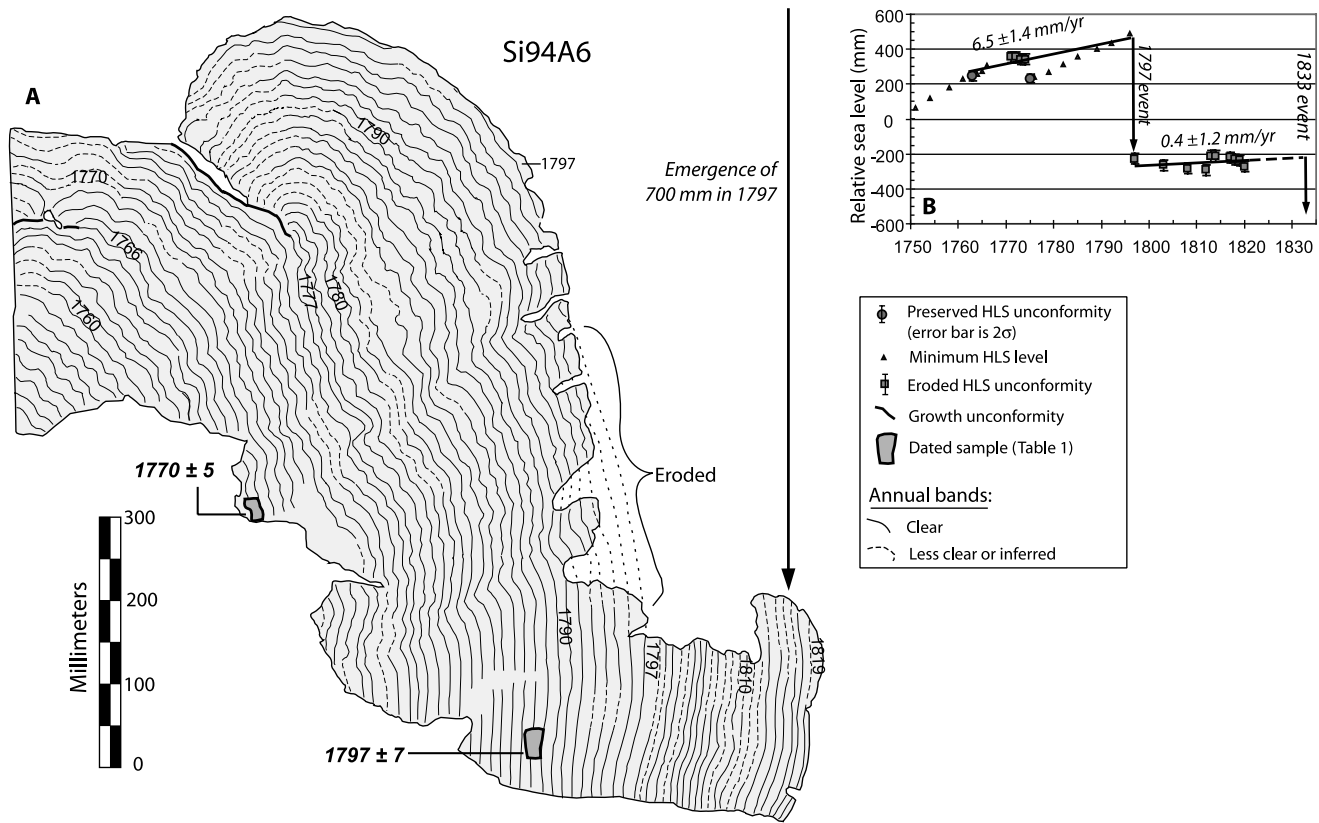


Figure 6. Stratigraphic analysis of slab Si94A6 (modified from Zachariassen *et al.* [1999], using U-Th dates in that paper). The dates of the annual rings are assigned so that a $\delta^{13}\text{C}$ anomaly in the thin outer bands coincides with 1815, the year of the eruption of Tambora in 1815 [Gagan *et al.*, 2000]. This gives the year 1797 as the last year during which thick annual bands formed. Hence the prominent 700-mm emergence probably occurred in 1797, the year of a large historical, tsunamigenic earthquake in west Sumatra.

microatolls is typical for living microatolls of these two genera [Natawidjaja, 2003]. This similarity implies that the fossil microatolls are contemporaneous and record the same emergence event. We slabbed one each of the *Goniastrea* and *Porites* fossil microatolls and a living *Porites* microatoll.

4.2.1. Living, Modern Head (Bkl03A3)

[39] The slabbed modern microatoll from the Bangkaulu site lives about 60 m offshore. It contains an excellent record of episodic rise of the HLS (Figure 10). The clear annual banding in the slab leaves little uncertainty in the

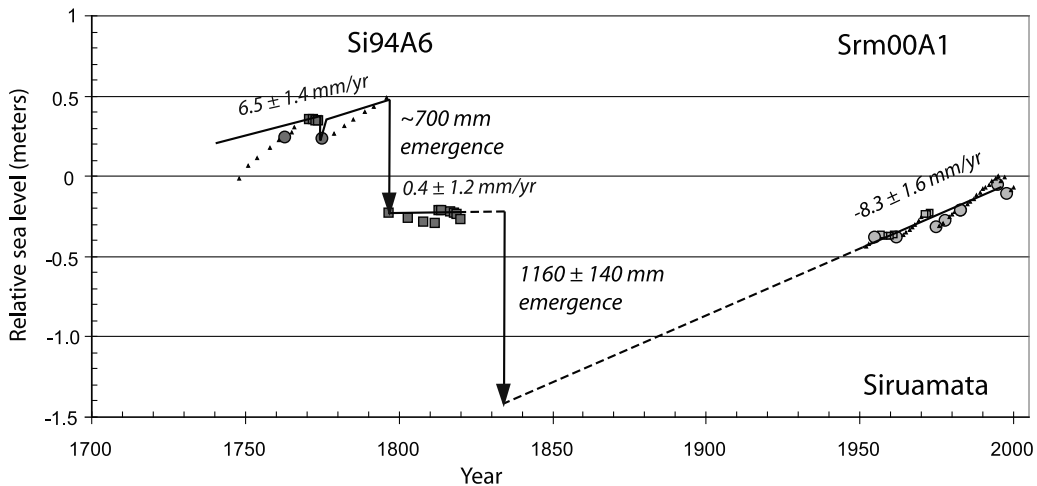


Figure 7. Combination of HLS histories from the fossil and modern heads at Siruamata that yields an estimate of about 1.2 m for coseismic emergence in 1833. Symbols are same as in Figure 6.

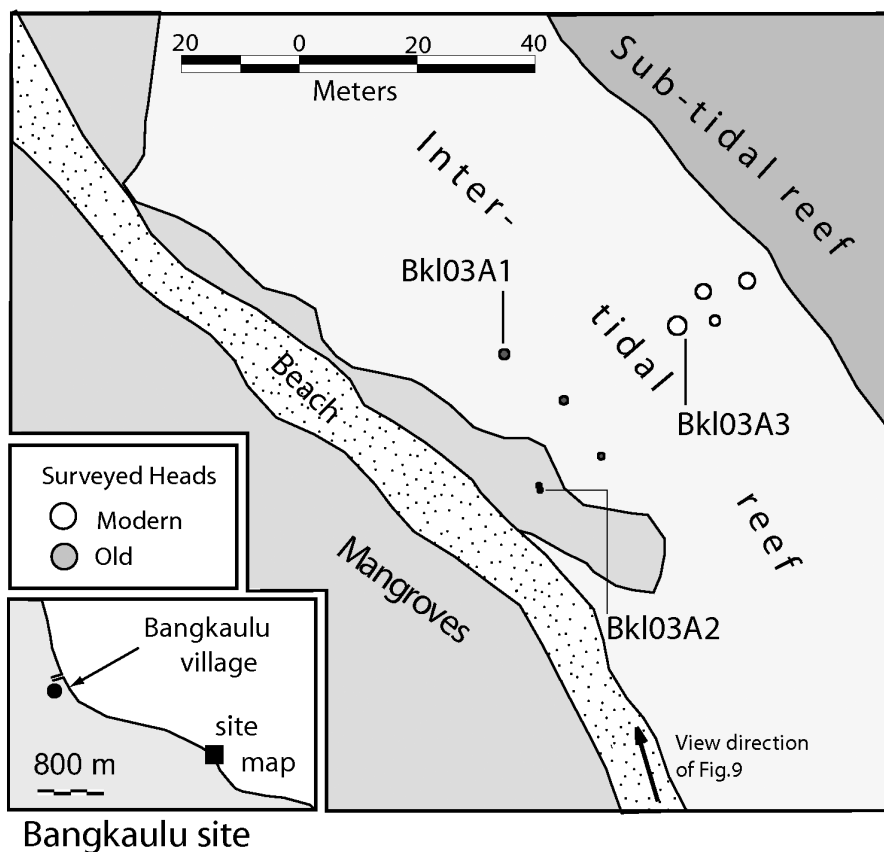


Figure 8. Map of the Bangkaulu site on southern South Pagai island. Two fossil heads (Bkl03A1 and Bkl03A2) and a modern head (Bkl03A3) constrain emergence in 1833 and show that no uplift occurred here in 1797. Between the site and Bangkaulu village, undated tsunami blocks up to 2 m in diameter are common.

assignment of dates to the bands, although only one of three U-Th dates from the slab are consistent with this visual counting (Table 1). Clear drops in HLS occurred during the El Niño years 1994 and 1997, as well as in about 1962 and 1979. The average rate of climb of the HLS between 1962 and 2002 is about 7 mm/yr.

4.2.2. Fossil Heads

[40] We slabbled one of the fossil *Goniastrea* microatolls (Bkl03A2), because this genus commonly has low initial ^{230}Th values that allow very precise and accurate dating. The location of this sample appears on Figure 8, but we do not include an illustration of the slab here. This slab yielded a date of A.D. 1800 ± 5 (Table 1) for a sample 80 to 250 mm in from the ragged outer edge of the microatoll. This supports the interpretation that the field of heads died in 1833, although the banding in the slab is too ambiguous to make an exact count of years between the sample and the death of the head.

[41] Sample Bkl03A1 is from a large *Porites* microatoll farther out to sea (Figure 8). We sampled this head because its large size promised a long pre-1833 HLS record. In fact the slab records HLS unconformities throughout the 7 decades prior to 1833 (Figure 11). The average rate of submergence prior to emergence in 1833 is about 6 mm/yr, statistically indistinguishable from the average modern rate.

[42] The U-Th dates from this fossil *Porites* microatoll show that it died in the late 18th or early 19th century. This is consistent with death in 1833, but the large uncertainties in the dates allow that death could have occurred in 1797. The low error in the date of the contemporaneous *Goniastrea* head, however, shows that the *Porites* micro-



Figure 9. Photograph of numerous small *Goniastrea* microatolls and mangroves near the beach at the Bangkaulu site. View is toward the northwest.

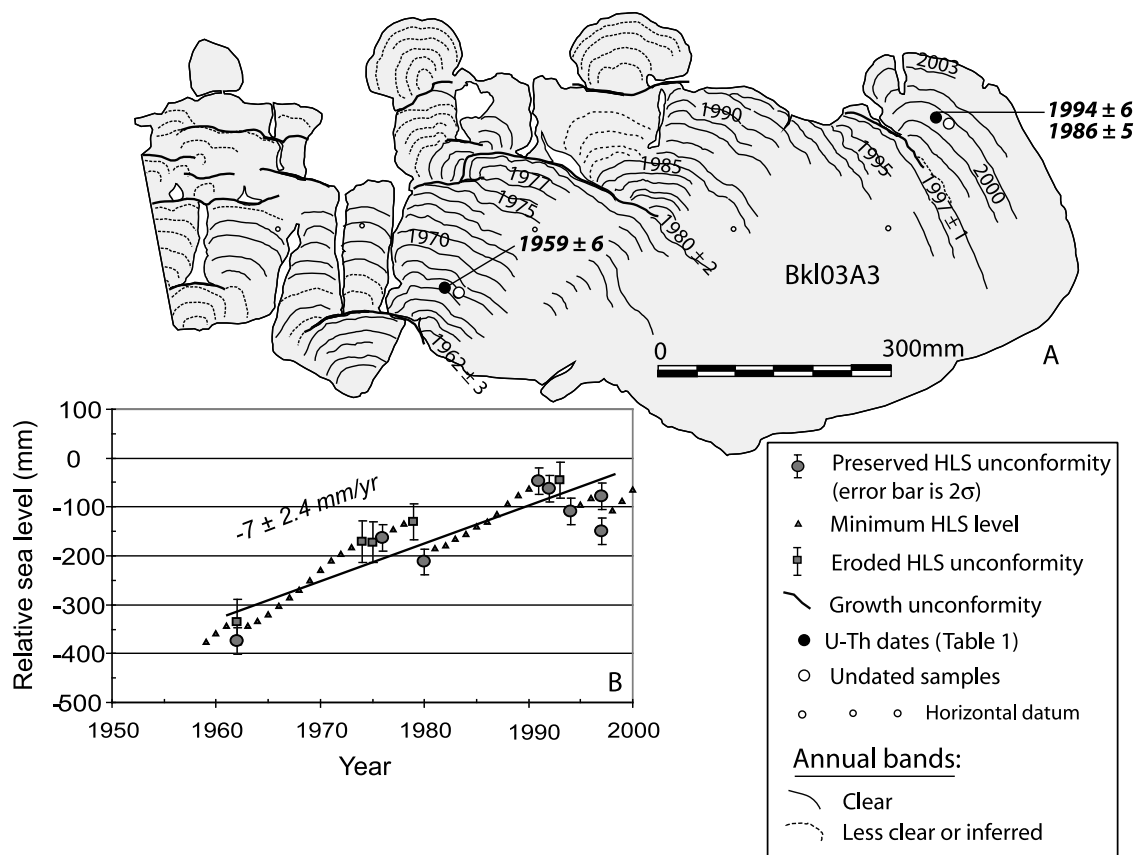


Figure 10. Modern history of sea level change revealed in microatoll Bkl03A3 at Bangkaulu. (a) Cross section showing clear HLS unconformities in about 1962, 1976, 1980, and 1990 and in the El Niño years 1994 and 1997. The small open circles (in this and other cross sections) are drill holes that preserve a record of horizontality during analysis. (b) Graph of HLS elevation versus time showing 4 decades of submergence at an average rate of about 7 mm/yr.

atoll most likely died within a few years of 1833, in which case the coral death likely resulted from emergence during the 1833 earthquake. The *Porites* microatoll record constrains any change in HLS in 1797 to be either null or slightly negative. In section 5.1.2 we show that this provides a crucial constraint on the southeastern extent of the fault rupture of 1797.

4.2.3. Emergence in 1833

[43] The HLS records of the modern and fossil heads constrain the magnitude of emergence in 1833 at Bangkaulu to about 1.8 m. The HLS elevation just prior to the 1833 event was about 0.5 m above HLS in 2003 (Figure 12). Extrapolation from the 2003 HLS back to 1833, using the average modern rate, yields an HLS elevation of about 1.3 m below the 2003 level. Under this assumption, the difference between immediately preearthquake and postearthquake elevations is about 1.8 m.

4.3. Sibelua Site (Sbl)

[44] The Sibelua site represents sites along the northeastern coasts of the Mentawai islands. It lies about halfway up the northeast coast of South Pagai (Figure 2). The setting is typical of the protected eastern side of the island in that it comprises labyrinthine waterways through mangrove swamps (Figure 13).

[45] We sampled both a living and a fossil microatoll at Sibelua. The living head sits on the seaward edge of the shallow reef; the fossil head is nestled within the convoluted margin of two stands of mangrove, against a border of mangrove snags. As is the case throughout the Mentawai archipelago, these dead tree trunks and roots testify to gradual submergence of the islands during the past few decades.

4.3.1. Analysis of the Modern Head

[46] The modern microatoll, Sbl02A2, shows episodic submergence, marked by 3- to 10-year-long periods of HLS stability interrupted by 10- to 15-year-long periods of uninhibited upward growth (Figure 14). It is odd that the HLS unconformities are not associated with El Niño years. The record reveals a 40-year average rate of submergence of about 6 mm/yr.

4.3.2. Analysis of the Fossil Head

[47] The fossil head that we sampled is representative of a family of large fossil microatolls whose tops are nearly concordant. These are most notable for their large diameters and hat shape; each has a raised central disk and a wide lower brim (Figure 15).

[48] In cross section the sampled microatoll displays a history of nearly a century of progressive submergence, prior to a prominent emergence (Figure 16). U-Th analyses show that this period spans most of the 18th century.

Figure 11

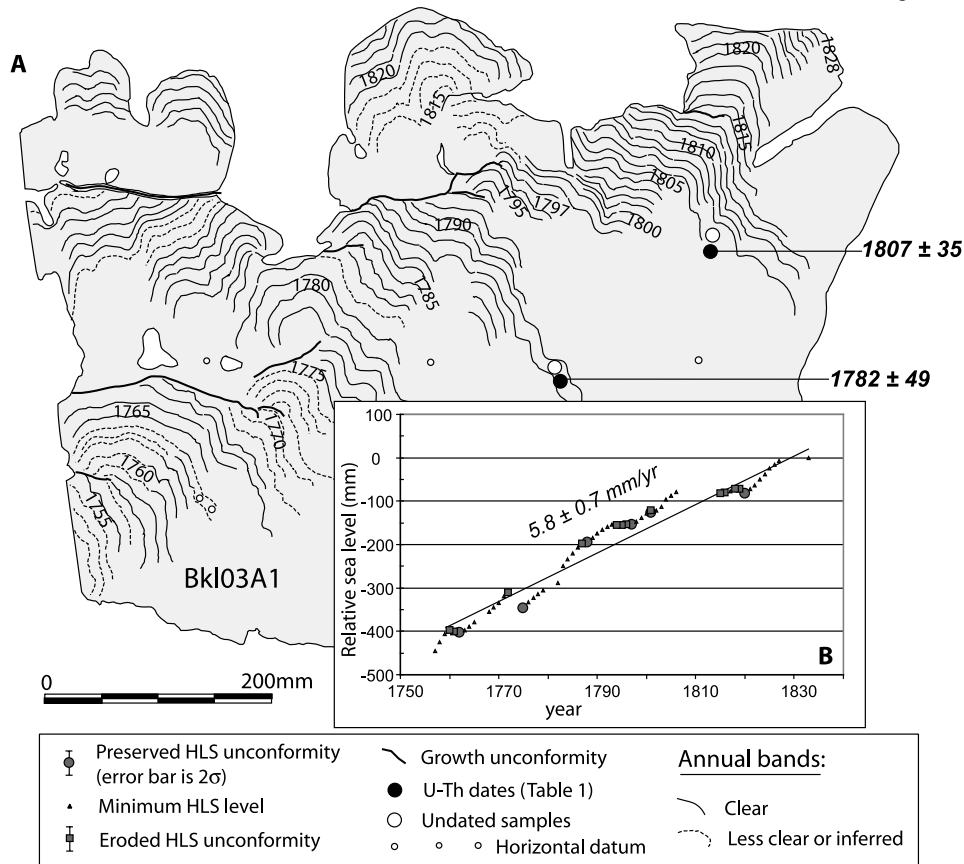


Figure 11. Pre-1833 history of sea level change revealed in fossil *Porites* microatoll Bkl03A1 at Bangkaulu. (a) Cross section showing rapid submergence through 7 decades in about the mid to late 18th century. U-Th dates yield averaged date of 1827 ± 28 for outermost band. Date of 1805 ± 5 on annual band in contemporaneous nearby *Goniastrea* head shows that this population died no sooner than 1815. Thus we assign dates of 1757 and 1770 to the major HLS unconformities because they are consistent with the dates of lesser tsunamigenic earthquakes. This is consistent with the U-Th dates and only 5 years or so of erosion of the perimeter if it emerged in 1833. The high quality of the annual bands in this sample leads to no uncertainty in band counting. (b) Graph of HLS history showing that the submergence rate averaged about 6 mm/yr during the 7 decades prior to 1833.

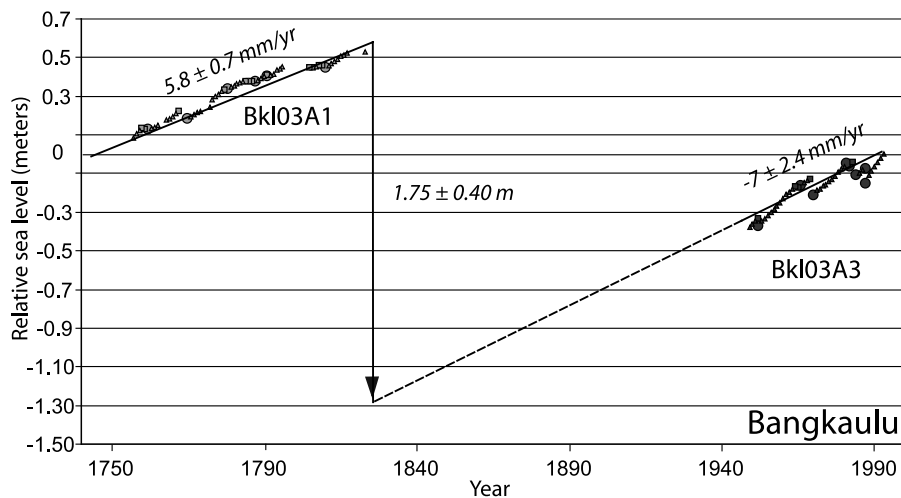


Figure 12. HLS time series at Bangkaulu showing that this site did not emerge during the 1797 event but rose about 1.8 m in 1833.

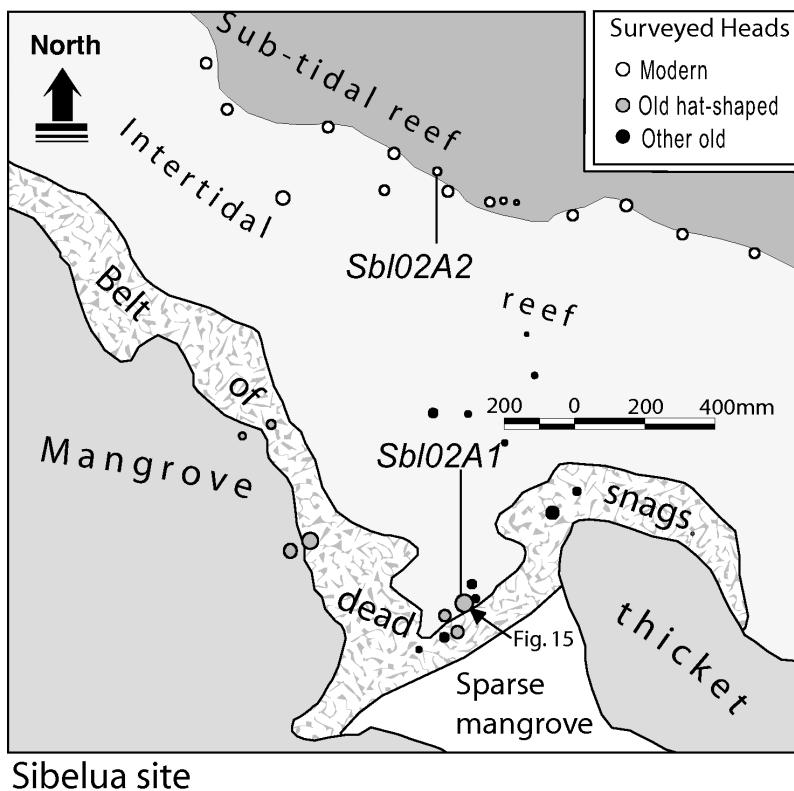


Figure 13. Map of the Sibelua site on the northeastern coast of South Pagai island. The belt of dead mangrove snags on the perimeter of the living forest is evidence of submergence over the past few decades. Fossil microatoll Sbl02A1 and modern microatoll Sbl02A2 yielded clear HLS time series. Arrow shows approximate view direction in Figure 15.

Several HLS impingements are well preserved between about 1717 and 1735. A deep HLS unconformity in about 1735 followed by about a decade of unimpeded upward growth suggests the occurrence of a minor emergence followed by a slightly larger submergence. Between 1735 and 1783, the tops of successive annual bands rise higher and higher but erosion has removed all but one indication of HLS impingement (in about 1770). Annual variations in HLS are commonly a few tens of millimeters, so erosion probably has been greater than that amount. However, the gradual, nearly linear slope along the top of this section of the head suggests that the slope reflects a long-term submergence at a rate of about 3 mm/yr between about 1745 and 1770.

[49] The tops of annual bands that formed between about 1783 and 1797 ostensibly imply a large, rapid drop in sea level over several years. However, the utter lack of evidence of HLS unconformities on these bands is a reason to be suspect of this interpretation. We suspect, instead, that about 20 cm was eroded off the side of the head after it emerged in 1797. The steep flanks of emerged heads are sometimes particularly susceptible to lateral erosion [Natawidjaja *et al.*, 2004], so this would not be an unusual case, although the amount of erosion would be several times more than appears on the head in Figure 6.

[50] HLS unconformities are also not preserved on the top of the outer flange, which grew between the 1797 and 1833 emergences. Nonetheless, the inward dip of the outer brim

indicates clearly that submergence at an average rate of about 4 mm/yr dominated the period between the two events.

4.3.3. Emergence in 1797 and 1833

[51] The HLS history inferred from the fossil and modern microatoll slabs implies coseismic uplifts in 1797 and 1833 of about 0.5 and 1.1 m, respectively (Figure 17).

[52] The height of the pre-1833 HLS is a few centimeters above the 2002 HLS. Extrapolation of the 2002 level back to 1833, using the average modern rate of about 6 mm/yr yields a post-1833 HLS a little more than 1.0 m below the 2002 level. Accordingly, we estimate the 1833 coseismic emergence to be about 1.1 m, the sum of these two values.

[53] The record of HLS in the fossil head constrains the magnitude of emergence in 1797 to about 0.5 m. Because we believe that the record of HLS rise in the 2 decades prior to 1797 has been obliterated by erosion, we must extrapolate the older record forward to 1797. This yields a preearthquake HLS about 0.3 m above the 2002 HLS. The immediately postearthquake HLS is constrained by the top of the 1797 ring to about 0.2 m below the 2002 HLS. Hence the magnitude of coseismic emergence in 1797 is about 0.5 m.

[54] The steep slope of the top of the five or six annual bands formed immediately after the 1797 emergence suggests a postseismic transient following the 1797 earthquake. During that period about 70 mm of the coseismic emergence was recovered by submergence (Figure 17).

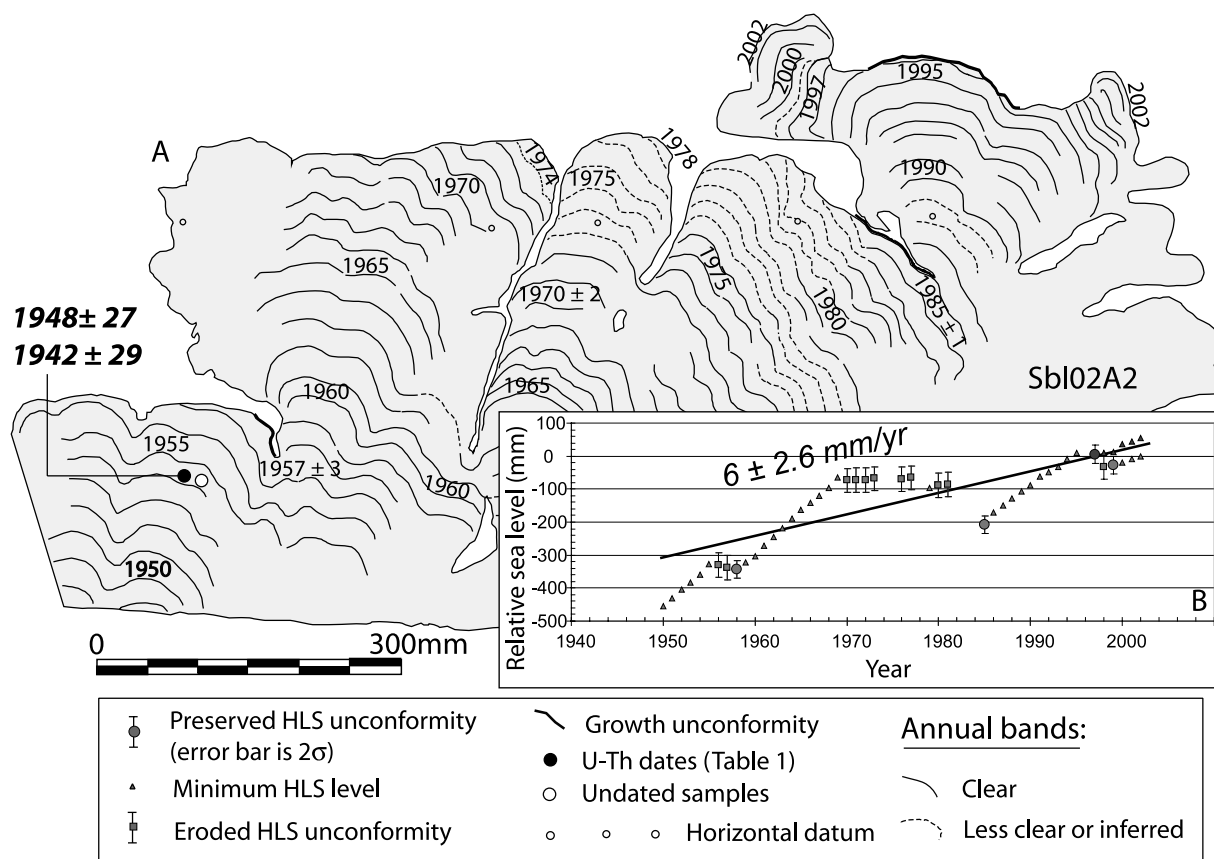


Figure 14. Modern history of sea level change revealed in microatoll Sbl02A2 at Sibelua. (a) Pattern of annual bands in cross section of modern head showing two periods of uninhibited upward growth between three periods of relative HLS stability. (b) HLS time series for the modern head at Sibelua that yields an average rate of submergence of about 6 mm/yr for the past 5 decades.

4.4. Pitogat Site (Ptg)

[55] The Pitogat site is the northernmost site on Sipora from which we have recovered clear evidence of the 1797 or 1833 event. The site is on the south side of a large bay near the western shoulder of Sipora island (Figure 2). Our data from Pitogat indicate that combined emergence of 1797 and 1833 was about 1.1 m.

[56] The coastline at Pitogat runs east-west and the intertidal reef is about 130 m wide (Figure 18). Immediately to the south is a narrow active beach, backed by a forested, inactive sandy back-beach slope. Snags rooted beneath the modern beach and on the nearshore part of the intertidal reef testify to recent submergence of the site.

[57] Fossil heads are concentrated along the southern 30 m of the intertidal reef and modern heads live in a band up to 40 m beyond these. We sampled one fossil and one modern head from these two populations.

[58] The HLS record contained in the modern slab is unusual in that it shows a clear reversal in the sense of vertical motion in the past 40 years. Unconformities in the record make interpretation of HLS changes prior to 1962 impossible (Figure 19a). Nonetheless, between 1962 and 1988, HLS clearly rises about 200 mm at an average rate of about 6 mm/yr (Figure 19b). The subsequent HLS trend has been downward, with HLS unconformities in 1990, 1994, and 1997. One could discount this reversal in trend as being

tectonically insignificant, given that both 1994 and 1997 were El Niño years of exceptionally low tides and that 1997 was also the year during which much of the fauna of the western Sumatran reefs died in association with the extensive Sumatran and Kalimantan fires [Natawidjaja et al.,

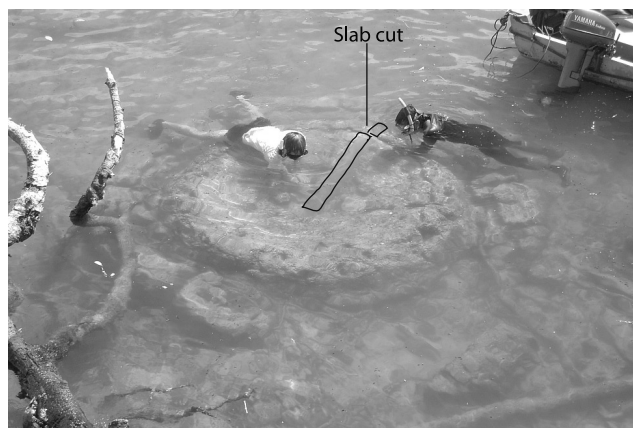


Figure 15. Photograph of fossil microatoll Sbl02A1 at Sibelua, from the boughs of a mangrove snag, showing the hat shape of the head, a raised central disk surrounded by a low outer brim. View is approximately toward the north-west.

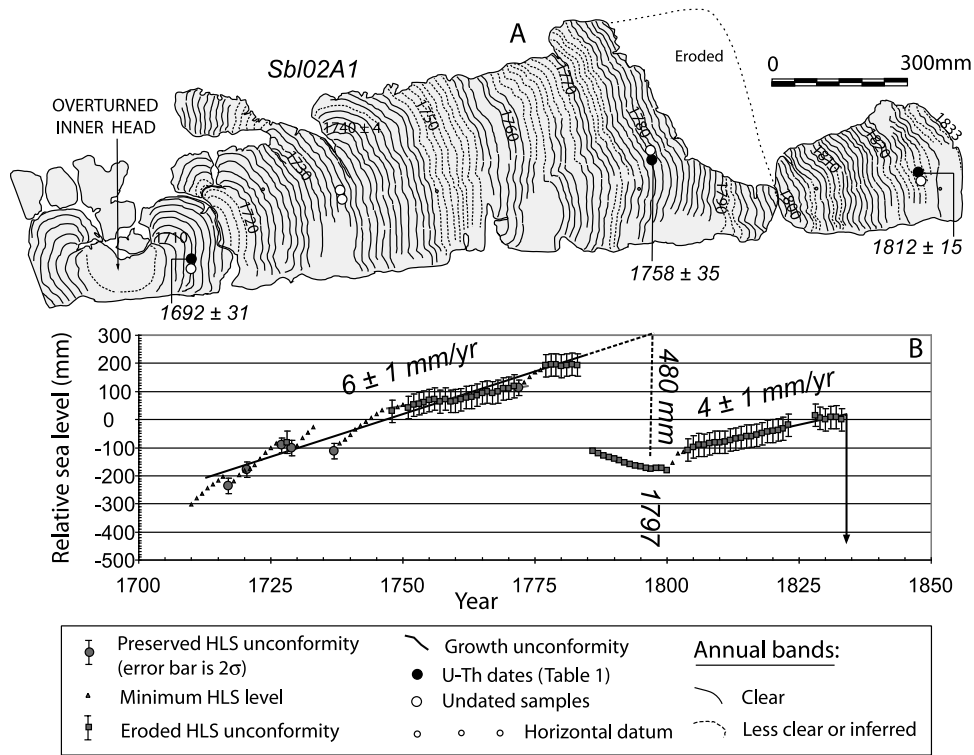


Figure 16. Fossil *Porites* microatoll Sbl02A1 that records more than a century of relative sea level changes at Sibelua before uplift in 1833. (a) Annual bands showing an abrupt emergence in the late 1700s, steady submergence in the decades before and after, and emergence in about 1833. The annual bands that formed in the 15 years before 1797 were partially eroded after emergence in 1797. U-Th date of 1812 ± 15 supports interpretation that final emergence and death occurred in 1833. (b) HLS time series showing rates of about 6 mm/yr before and 4 mm/yr after emergence late in the 1700s.

2004]. However, the HLS unconformity in the non-El Niño year of 1990 suggests the reversal may be of tectonic origin. Below, we use the average rate from 1962 to 1988, about 6 mm/yr, in calculating the emergence associated with the 1797 and 1833 events. If we were to include the later HLS values, the amounts of emergence calculated below would be about 0.2 m lower.

[59] The fossil microatoll at Pitogat has the classic morphology of heads on a submerging coast, a lower central

flat formed in 1745 is surrounded by several terrace rings that are progressively higher toward the head's perimeter (Figure 20a). The cross section shows these as five distinct erosional unconformities, on the tops of annual bands formed in 1753–1754, 1759, 1765–1770, 1780–1783, and 1789 (Figure 20b). U-Th analyses show that the head grew during the decades between about 1740 and 1790.

[60] The HLS dropped nearly 100 mm in about 1770. This may be tectonically significant, since the cross section

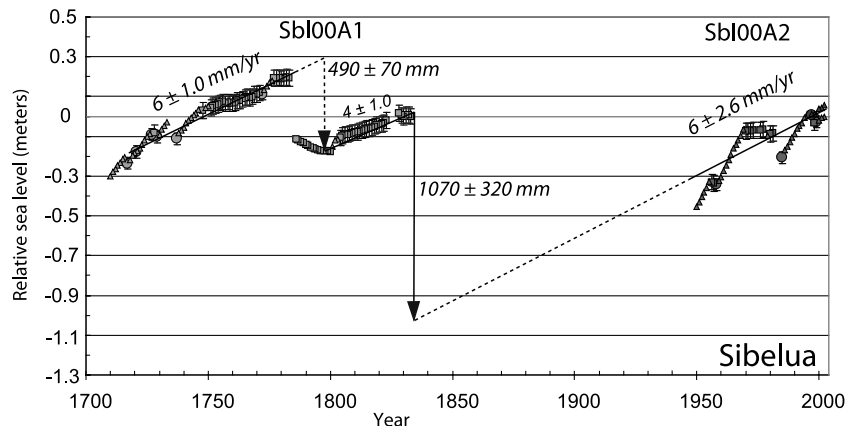


Figure 17. HLS time series from modern and fossil microatolls at Sibelua showing 0.5-m uplift in 1797 followed by 1.1-m uplift in 1833.

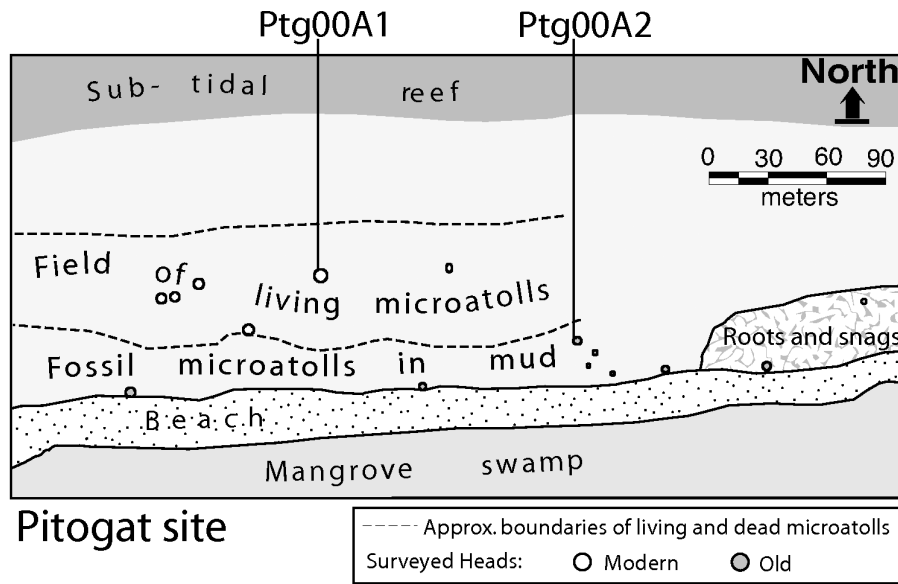


Figure 18. Map of Pitogat site on northwestern flank of Sipora island showing the classic marks of an oscillating sea level. The beach has transgressed over the muddy and peaty substrate of the swamp, in which mangrove snags are rooted. Fossil heads that underlie the peat and mud indicate that uplift raised the heads above their HLS. We cut samples of modern microatoll Ptg00A1 and fossil microatoll Ptg00A2.

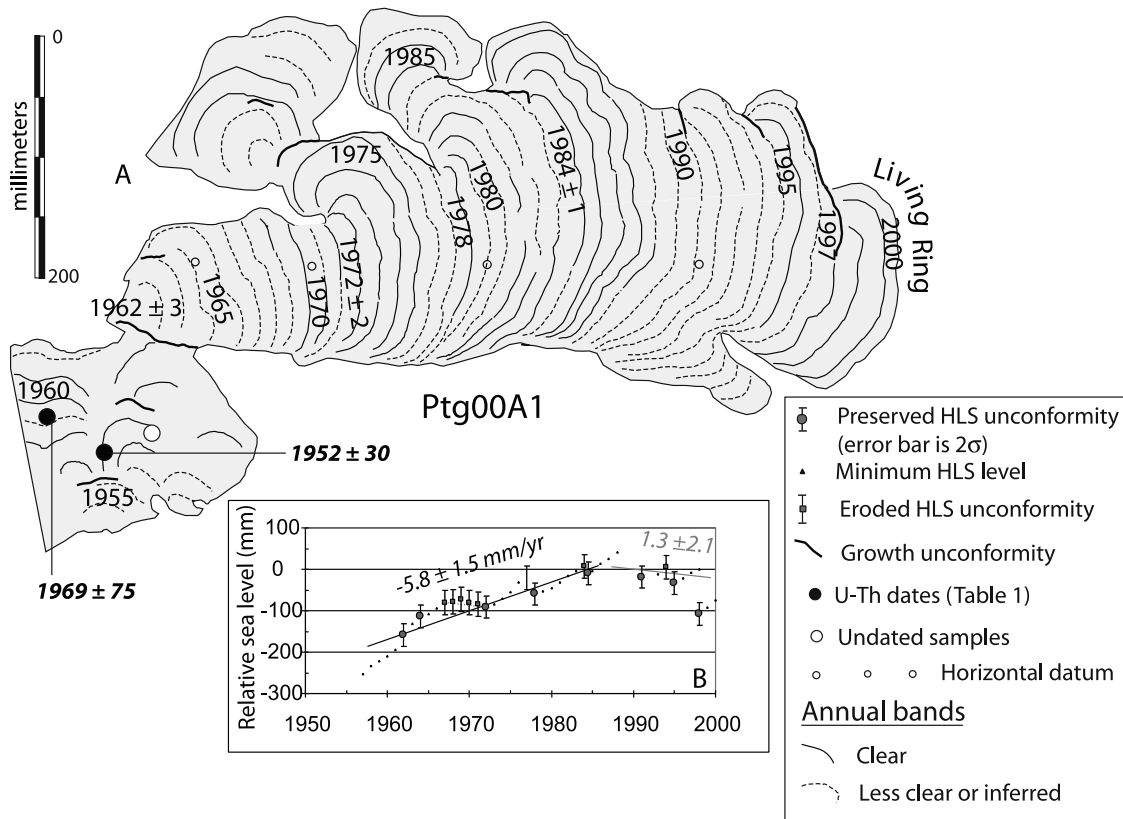


Figure 19. Modern history of sea level change revealed in microatoll Ptg00A1 at Pitogat site. (a) Annual bands in vertical, radial cross section showing submergence followed by emergence. Unconformities in the oldest part of the head obscure HLS history prior to 1962. (b) Graph of modern HLS history. Rise of HLS at about 6 mm/yr began in 1962 and continued until 1988. Since 1988, HLS has been nearly stable, except for the prominent die-down of the living perimeter during the regionally extensive death of Mentawai and Batu islands' reefs in 1997.

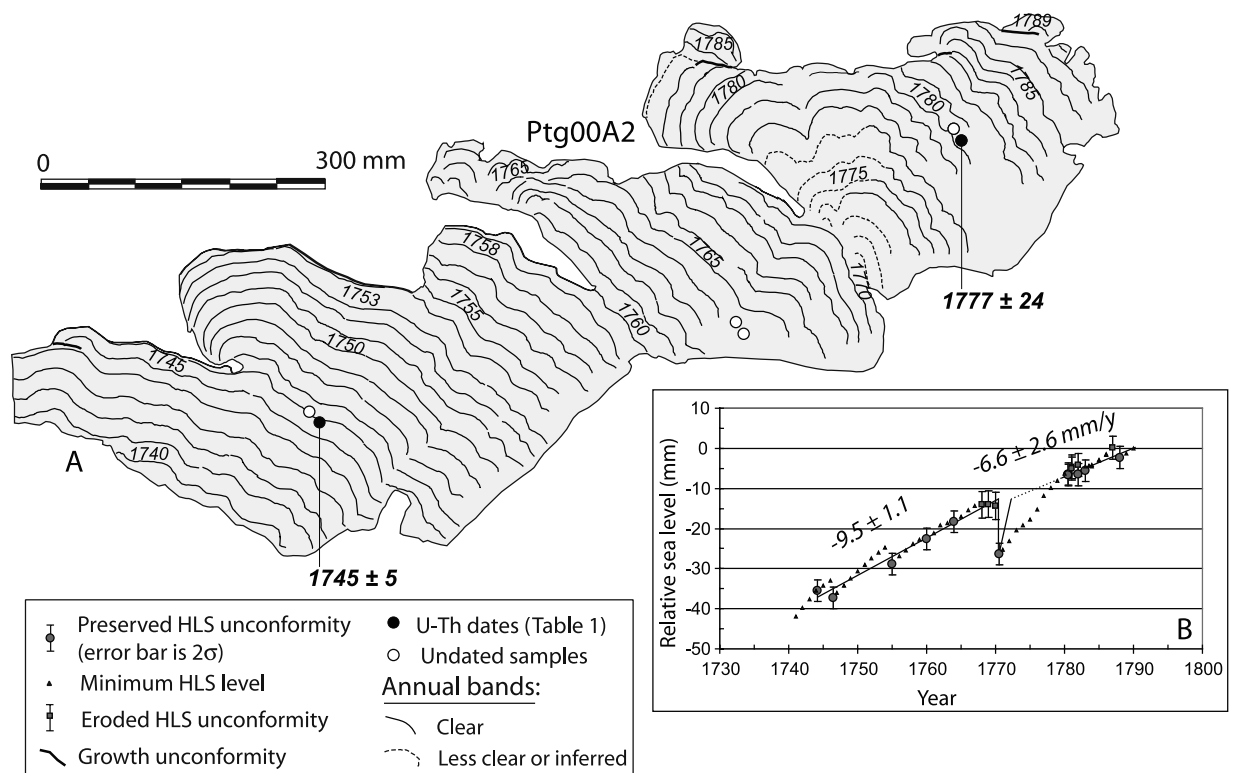


Figure 20. Pre-1797 history of sea level change revealed in fossil *Porites* microatoll Ptg00A2 at Pitogat site. (a) Cross section of fossil head. This head grew during the last 6 decades of the 18th century and probably died because of emergence in 1797. The two most prominent HLS unconformities in the record may have occurred in the years of two historically known tsunamigenic earthquakes, 1756 and 1770. U-Th date of 1745 ± 5 near center of microatoll implies a date of about 1789 for the outermost ring, consistent with several years of erosion after uplift in 1797. (b) HLS time series for Pitogat site showing submergence at high rates throughout the last half of the 18th century.

shows that corallites growing lower on the perimeter of the microatoll in 1770 also died at this time. If this was due to an influx of sand that buried and killed the lower edge of the microatoll, it may have been related to the historical tsunamigenic earthquake of 1770 [Newcomb and McCann, 1987].

[61] Because the fossil microatoll sat within the intertidal zone until recent submergence carried it back below lowest low tides (Figure 21), the submergence of the 18th century must have given way to emergence sometime after about 1790. The modern record at Pitogat constrains this emergence to a time well before 1962. One simple interpretation is that the emergence was associated with the 1797 event, since the head died soon after about 1790 (Figure 20b). However, a mere 20 cm of emergence in 1797 would have killed the head, since its outermost annual band is so thin. The remainder of the emergence could have occurred in 1833. Extrapolation of the fossil record forward in time from the 1700s and the modern record back yields an estimate of about 1.1 m of emergence during one or both of these events (Figure 21). This ambiguity in the partitioning of the emergence will remain until recovery of a head that captures the HLS level just after the 1797 event.

4.5. Remaining Sites

[62] In addition to the four sites just described in detail, ten others display evidence for uplift in 1797 or 1833 or

both. In the interest of brevity, we summarize the data for these sites, below, rather than elaborating them fully. Details from the first three of these ten sites (Singingi, Silabu and Silogui) appear in the auxiliary material (Text S2). The next three sites (Simanganya, Sikici, and Bulasat/Saomang) contain evidence not only for these most recent emergences but also for prior large emergences. They will be examined in detail in a separate, forthcoming paper on the recurrence of large ruptures beneath the Mentawai islands. The Badgugu site, in the Batu islands just south of the equator, contains a continuous 250-yearlong record of relative sea level, the longest obtained from any site in western Sumatra. It will be the centerpiece of a future paper on the long-term behavior of the largely decoupled section of the megathrust near the equator. The Tiop bay, Siatanusa and Tinopo island sites, were examined in detail by Zachariasen *et al.* [1999] and hence require only brief review.

4.5.1. Singingi Site (Sgg)

[63] This locality is on the northern tip of a swampy mangrove islet off the northeast coast of South Pagai (Figures 2 and S1). A fringe of dead snags rooted in the intertidal reef flat bears witness to the fact that the islet is slowly submerging (Figure S2). We collected slabs from two fossil microatolls and one living microatoll to define the HLS history of the site (Figures S3–S5).

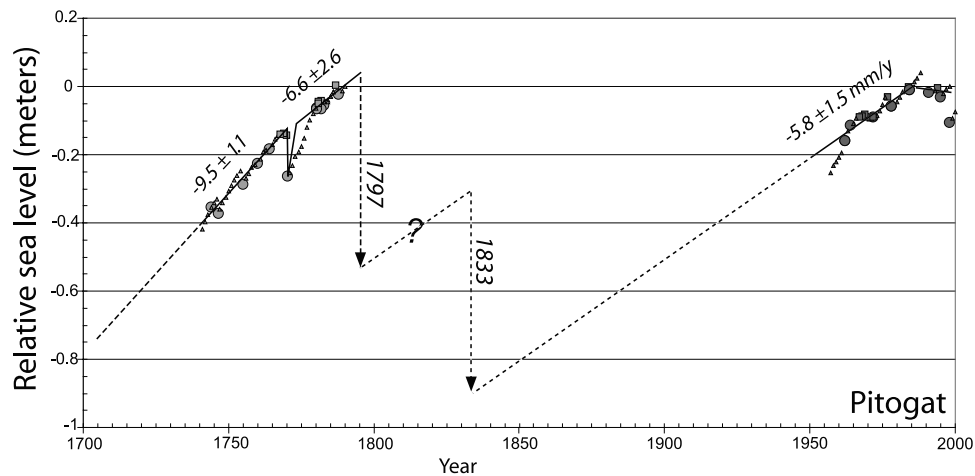


Figure 21. HLS time series for Pitogat site, eastern Siberut island. Combined emergence associated with the 1797 and 1833 events is about 1.1 m. Lacking additional constraints, the nature of partitioning of slip between the 1797 and 1833 events is uncertain.

[64] Figure 22f is a composite of the HLS records of the three slabs from Singingi. The relationship between fossil heads Sgg03A1 and Sgg03A2 shows that at least the 18th century part of head Sgg03A2 has been eroded substantially. Together the three heads yield an estimate of about 0.4 m for emergence in 1797. The difference between the pre- and post-1833 HLS is about 1.5 m.

4.5.2. Silabu Site (Slb)

[65] This site is on the west coast of North Pagai island, on the south side of a large bay, about 95 km from the trench (Figure 2). The locality was first studied extensively by Zachariassen *et al.* [1999], who found clear evidence for uplift in 1833 and during an event a few decades earlier. Two distinct populations of fossil microatolls populate the intertidal reef platform (Figure S6). The outer raised rims of the older population commonly are about 0.8 m higher than those of the lower population.

[66] A modern slab (Figure S8) and several slabs from the fossil populations (Figures S9–S12) constrain HLS between about 1710 and 1833 and allow us to document HLS history of the past 2 decades (Figure 22e). Together these records show that emergence was about 0.8 m in 1797 and about 2.2 m in 1833.

4.5.3. Silogui Site (Slg)

[67] Silogui is the northernmost site in the Mentawai islands from which we have evidence of the 1797 or 1833 event (Figure 2). The site is near the mouth of a long, narrow bay on the east coast of Siberut island. We recovered a fossil microatoll from the site (Figure S14) and measured the elevation of living HLS on (but did not slab) a modern head. For a surrogate modern submergence rate, we used the rate calculated from a slab collected at Teluk Saibi, about 6.5 km to the south. As at Pitogat, the microatoll indicates that combined emergence in 1797 and 1833 was about a meter (Figure 22b). The top of the fossil head is about 100 mm below the modern 2002 HLS. At 5 mm/yr, the net submergence since 1788 should have been a little over a meter. One or more emergence events between 1788 and the present would be required to raise the head that amount, and 1797 and 1833 are the best candidates.

4.5.4. Simanganya Site (Smy)

[68] Three adjacent sites along the northeastern coast of North Pagai island are near the town of Simanganya. Together they contain a 700-year-long record of several large emergence events. Figure 22d displays the portion of this composite record relevant to the 1797 and 1833 events. No clear disturbance of HLS appears to occur in or near 1797. Modern and fossil heads constrain emergence in 1833 to be about 1.8 m.

4.5.5. Sikici Site (Skc)

[69] The Sikici site is on the east coast of Sipora island. Like Simanganya, its record is a composite from three neighboring sites that spans the past seven centuries. Slabs cut from a fossil and a modern microatoll constrain the HLS history of the past three centuries (Figure 22c). Interseismic submergence has occurred at about 4 mm/yr throughout that period. The head does not record emergence in 1797 well, because it was experiencing unimpeded upward growth in the years before 1797, HLS dropped down about 40 mm below the top of the previous year's annual band. Thus emergence in 1797 could have been 40 mm or greater. In contrast, emergence in 1833 is well constrained by the modern and fossil heads to about 1.3 m.

4.5.6. Bulasat/Saomang Site (BlS/Smg)

[70] These neighboring sites on the west coast of South Pagai island contain a composite partial record of emergence events and interseismic submergence that extends about two millennia into the past. Combining the record from two fossil microatolls at Saomang with that of a modern head at Bulasat allows estimation of emergence in 1797 and 1833 (Figure 22g). One of the slabs (P96F1) contains a record of the 1833 event from a *Goniastrea* microatoll collected by Zachariassen *et al.* [1999]. The other (Smg02A2) is from a *Porites* microatoll that we collected. Together these constrain uplift in 1797 to be about 0.95 m. A slab from a modern microatoll at Bulasat, a few km to the northwest provides the elevation of the HLS in 2002. Its very rapid average modern rate of submergence extrapolates to a post-1833 HLS about 2.2 m below modern HLS. From this evidence we estimate an emergence of about 2.4 m in 1833, one of the largest values obtained among all our sites.

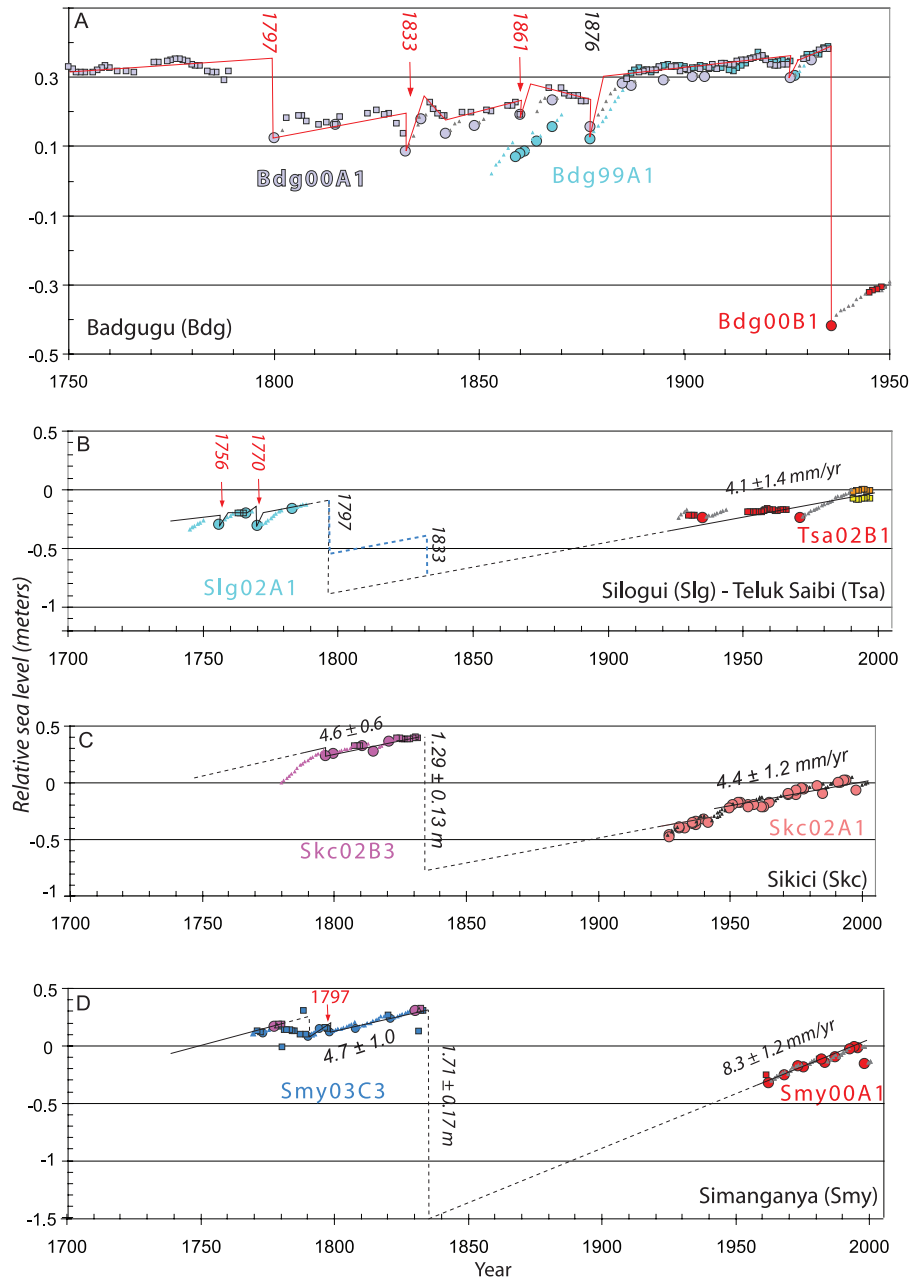


Figure 22. HLS histories for 10 sites not discussed in detail in this paper (see Figure 2 for locations). These records place important constraints on vertical deformation associated with the 1797 and 1833 earthquakes. (a) Badgugu (Bdg, southern Batu islands). (b) Silogui (Slg, northeast coast Siberut). (c) Sikici (Skc, northeast coast Sipora). (d) Simanganya (Smy, northeast coast North Pagai). (e) Silabu (Slb, west coast of North Pagai). (f) Singingi (Sgg, northeast coast South Pagai). (g) Bulasat/Saomang (Bls and Smg, southwest coast South Pagai). (h) Tiop bay (Ttp, southwest South Pagai). (i) Tinopo islet (Tnp, southern South Pagai archipelago). (j) Siatanusa islet (Stn, southern South Pagai archipelago). Data supporting Figures 22b, 22e, and 22f are given in the auxiliary material. History after 1935 in Figure 22a is from *Natawidjaja et al.* [2004]. Time series in Figures 22h, 22i, and 22j are from data of *Zachariasen et al.* [1999]. Use of multiple colors indicates HLS time series from different microatolls or different parts of the same microatoll at a site. Time series P96F1 in Figure 22g is corrected downward 100 mm because it is an HLS record from a *Goniastrea* microatoll; *Goniastrea* HLS is about 100 mm higher than *Porites* HLS (Appendix B).

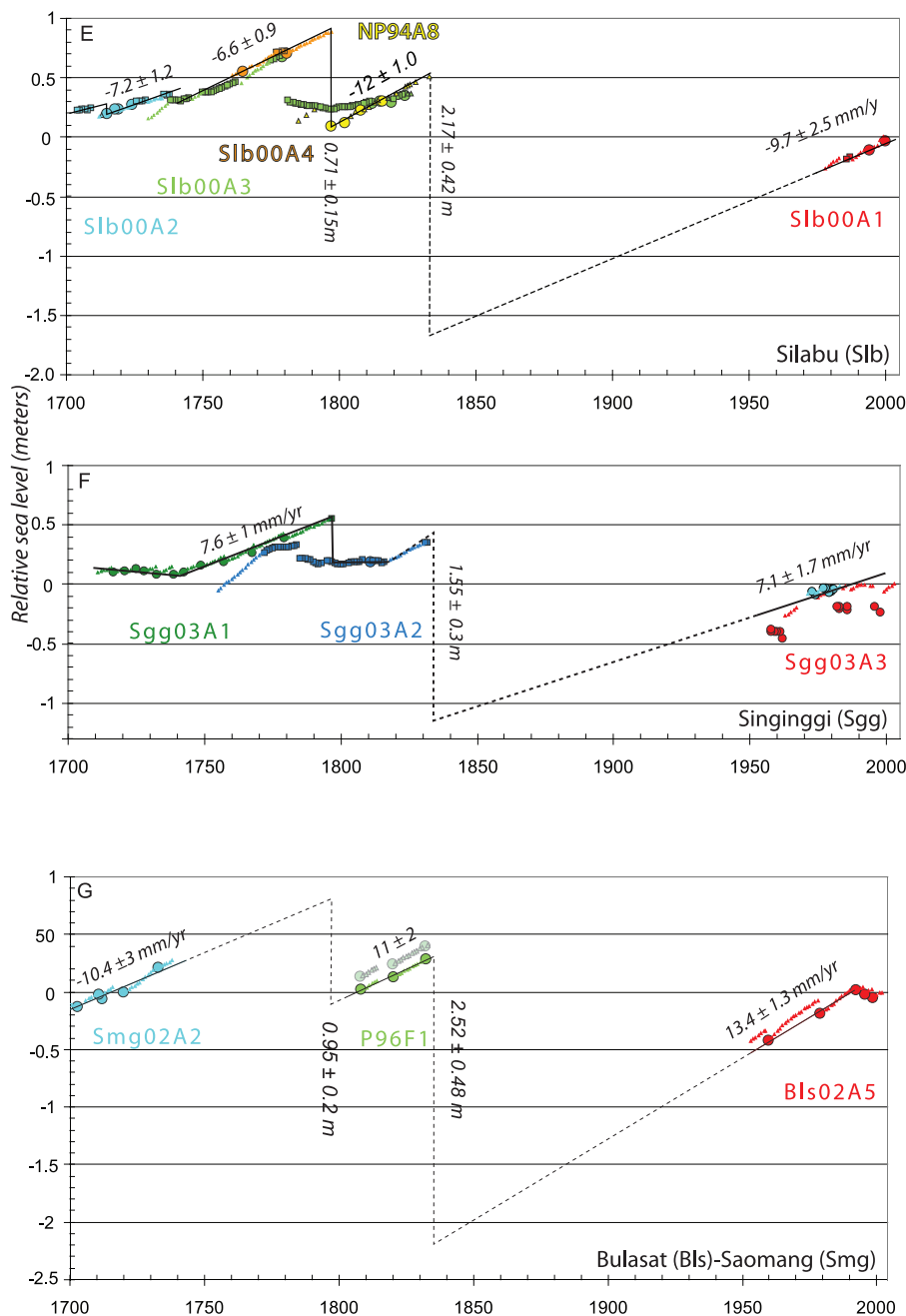


Figure 22. (continued)

If instead the average rate over the past 170 years were, say, 10 mm/yr, our estimate of coseismic uplift in 1833 would diminish to about 2 m.

4.5.7. Badgugu West (Bdg)

[71] The exceptionally long record from the Badgugu site (Bdg, Figure 2) places constraints on the northern extent of the 1797 and 1833 ruptures. One thin, flat microatoll there records HLS history from about 1746 to 1935 (Figure 22a). The head records an emergence in 1797 of about 200 mm. A rapid submergence of 50 mm follows within no more than 3 years. The microatoll records a small but clear emergence of about 100 mm in 1833, as well. This is followed by a submergence of about the same magnitude within no more than 5 years.

4.5.8. Three Sites From Zachariassen et al. [1999]

[72] Many localities in the Mentawai islands have microatolls whose deaths were dated to about 1833 by Zachariassen et al. [1999]. They collected slabs for HLS analysis at three of these sites, all on southern coasts of South Pagai island.

4.5.8.1. Tiop Bay (Ttp)

[73] Tiop bay is an elongate reentrant of the sea on the southern coast of South Pagai. A slab cut there by Zachariassen et al. [1999], P96H1, contains a record extending back about 60 years from 1833. The slab exhibits an emergence of only a centimeter or two in 1797 (Figure 22h). Because they did not slab a modern head at this site, they used a 7 mm/yr rate from a modern head 40 km to the

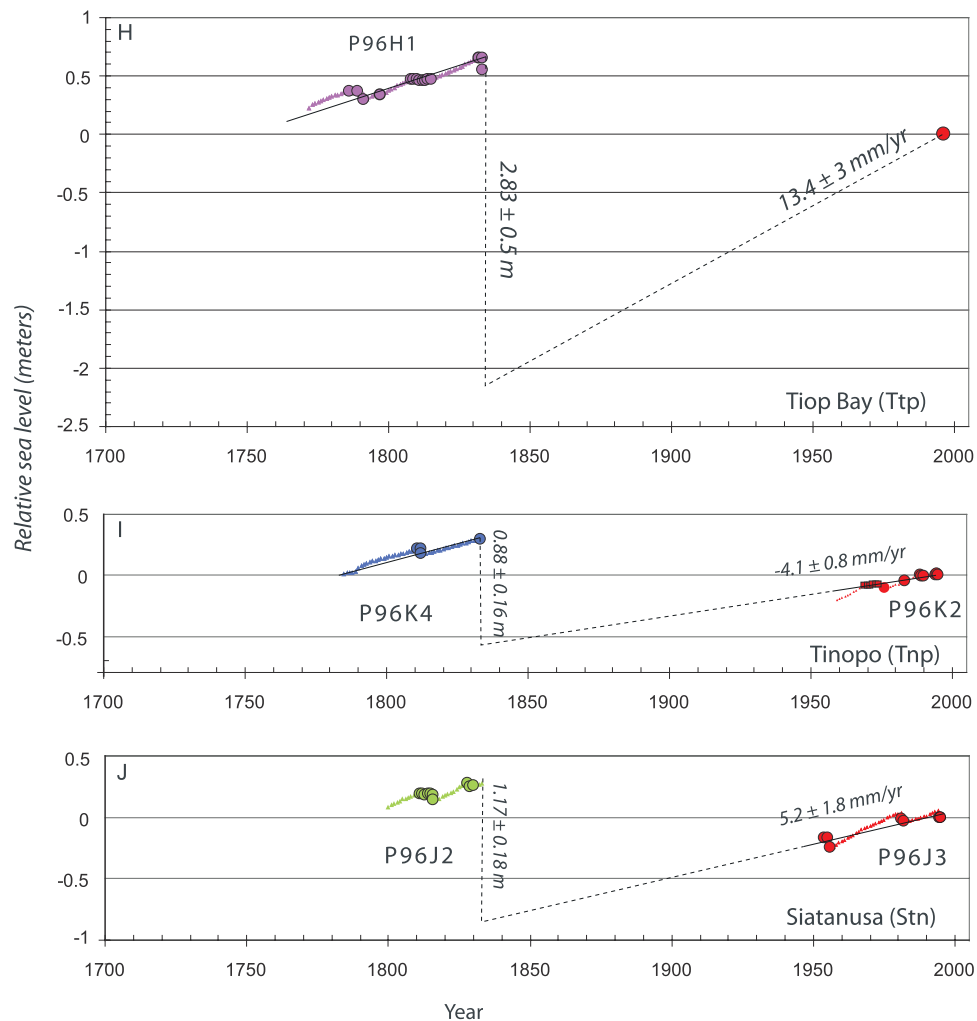


Figure 22. (continued)

northwest to estimate a 1.8-m 1833 coseismic step. We recalculated the coseismic step using the modern rate from Bulasat, about 10 km to the northwest and at about the same distance from the trench as Tiop bay. Because the modern rate at Bulasat is much faster (13 mm/yr, Figure 22g), we estimate a greater 1833 coseismic emergence, about 2.8 m. This is the largest known emergence associated with the 1833 earthquake.

4.5.8.2. Siatanusa (Stn) and Tinopo (Tnp)

[74] Both of these sites are from islets in the archipelago off the southeast coast of South Pagai. Zachariasen *et al.* [1999] cut two slabs at each site, one from a fossil and one from a living microatoll. Each modern slab yielded a record of submergence at average rates of about 4 to 5 mm/yr for the past 3 to 4 decades. U-Th dates of each fossil slab are consistent with death by emergence in 1833, but neither slab extends far enough into the previous decades to place a direct constraint on the effects of the 1797 event (Figures 22i and 22j). The slab from Tinopo, however, does include annual rings from as early as about 1785 (Figure 22i), but the first time upward growth is limited by HLS is in about 1810. Although this is not a direct indication of vertical

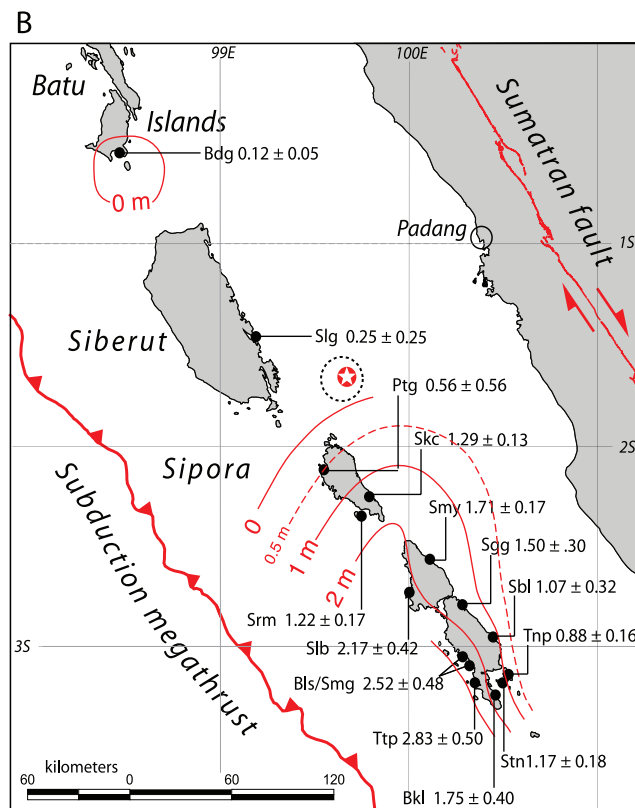
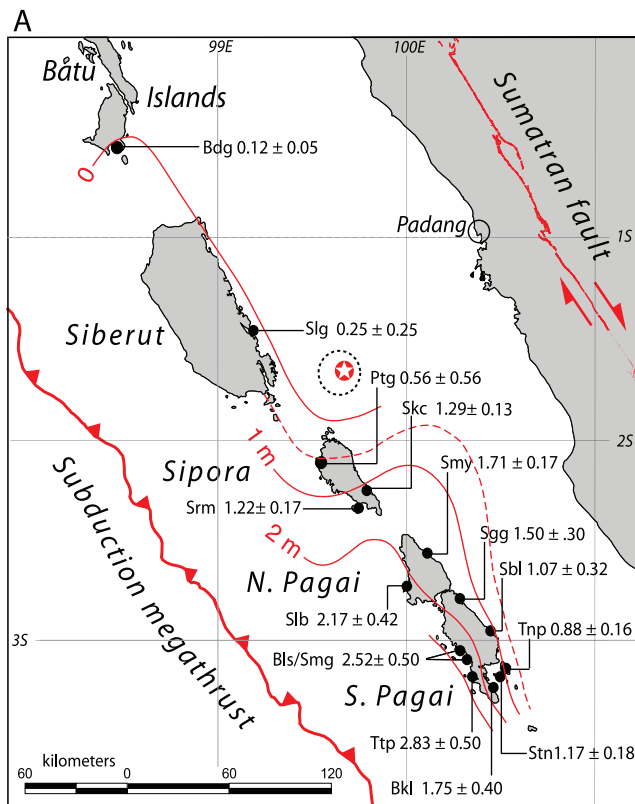
deformation in 1797, it does constrain the magnitude of emergence to no more than about 50 mm.

5. Discussion and Modeling

5.1. Synthesis of the Paleoseismic Records

5.1.1. Pattern and Magnitude of Uplift in 1833

[75] The record of microatoll emergence on the islands of the outer arc ridge places new constraints on the sources of the 1797 and 1833 earthquakes and tsunamis. Taken together, nine sites show that the Pagai islands tilted toward the mainland in 1833 (Figure 23). The pattern is coherent: Sites on or near the southwestern flanks of the islands rose 2.2 to 2.8 m, while sites on the northeastern coasts rose between 0.9 and 1.7 m. The tilt is markedly steeper in the south than in the north. The 1833 contours give no indication of closing toward the southeast, so emergence and tilt must have continued in that direction beyond South Pagai. This is consistent with the historical record of severe shaking and tsunami damage at Bengkulu (Appendix A), which suggests that rupture extended at least as far south as about 5° S.



[76] The similarity of uplift values at Siruamata and Sikici, on the southwest and northeast coasts of southern Sipora island (Srm and Skc on Figure 23), require a significant bending of the tilt axis across that island, and an appreciable northwestward diminishment of uplift across the island. The even lower value of 1833 emergence at Pitogat (northern Sipora island, Ptg, Figure 23) confirms the northwestward decrease across Sipora in 1833.

[77] Whether or not the uplift of 1833 reached Siberut is unresolved. If some portion of the uplift measured at Silogui occurred in 1833, then 1833 uplift extends some distance farther to the northwest, albeit with a distinct kink in contours in the strait between Siberut and Sipora, perhaps as depicted in Figure 23a. Another viable interpretation is that none of the emergence measured at Silogui occurred in 1833. In that case 1833 uplift would have ended near the south coast of Siberut, perhaps as depicted in Figure 23b.

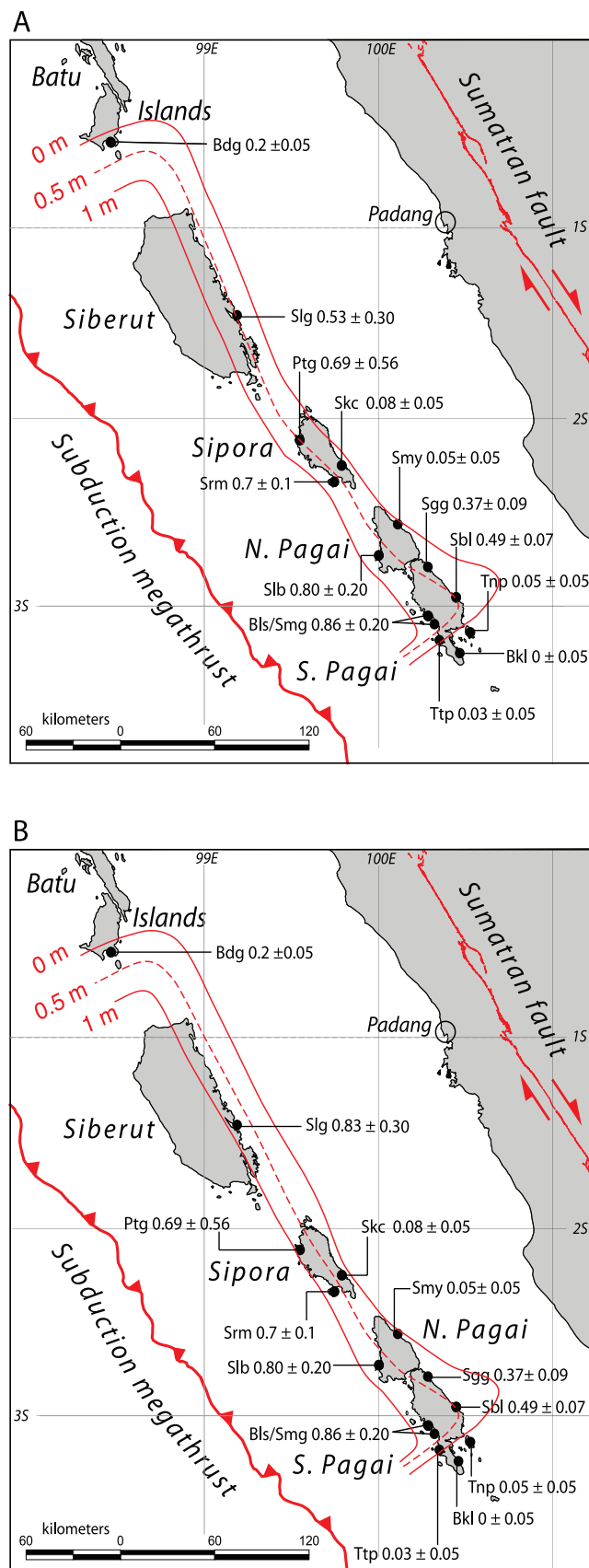
[78] Any partitioning of the 0.83 m of uplift measured at Silogui (Siberut) between the 1797 and 1833 events is plausible, as long as the uplift in 1797 is at least 25 cm, the thickness of the outermost annual band of the fossil microatoll there. However, given the near-zero value for 1833 emergence at Badgugu, we favor partitions that assign only a small portion to the 1833 event. In Figure 23a we allocate to 1833 slightly less than half of the uplift at Silogui and allow 1833 uplift to be contiguous all the way to Badgugu. In Figure 23b we give it none and assume that the very slight emergence at Badgugu was isolated from the main region of uplift.

5.1.2. Pattern and Magnitude of Uplift in 1797

[79] Ten sites on Sipora and the Pagai islands constrain the pattern of emergence in 1797 (Figure 24). The Pagai islands tilted northeastward, toward the mainland, but uplift was not as great as in 1833. On the southwestern coasts, uplift ranged between 0.7 and 0.8 m, and on the northeastern coasts it reached values as great as 0.5 m. The magnitude of uplift of Siberut in 1797 depends on how one partitions slip between 1797 and 1833 at Pitogat and Silogui. In Figure 24a, we tentatively ascribe a little more than half of the 0.83 m at Silogui to 1797, because the 1797/1833 emergence ratio is high farther north, at Badgugu. In Figure 24b, we ascribe all uplift measured at Silogui and more than half of the uplift at Pitogat to 1797.

[80] The southern limit of emergence in 1797 is delimited by the sharp southeastward decline in values across the southeastern end of South Pagai island. No emergence occurred at Bangkaulu (Bkl, Figure 24) in 1797, and at Tiop bay (Ttp) uplift is a mere 30 mm or so. However, only 15 km or so up the coast at Bulasat and Saomang (Bls/Smg), uplift appears to be about 0.8 m. If we have over-

Figure 23. Maps of uplift associated with the 1833 earthquake showing that a large region was raised between 1 and 2 m. A prominent feature is the tilt of the islands toward the northeast. Emergence (a) diminished greatly or (b) ended toward the northwest in the strait between Sipora and Siberut islands. The coral data do not constrain the southeastern limit of emergence. Star shows location of 10 April M_w 6.8 aftershock of the 28 March 2005, Nias-Simeulue earthquake. Dashed circle outlines region of aftershocks of that earthquake.



estimated the emergence at Bulasat/Saomang (i.e., if the modern submergence rate overestimates the average rate since 1797) then this gradient would be less steep, but still present.

5.2. Elastic-Dislocation Modeling of the Ruptures

[81] The ambiguities at Silogui and Pitogat and the lack of other sites on or near Siberut permit two basic uplift scenarios for 1797 and 1833. The difference between the two is that 1833 uplift in one scenario extends beneath Siberut and in the other it does not. We favor the latter, for three reasons. First, all contouring of the 1833 data that is faithful to the three measurements on Sipora require, at the very least, a sharp bend in the 1833 uplift contours and a northwestward lessening of uplift (Figure 23a). The northwest diminishing uplift allows drawing of the zero uplift contour through the Sipora/Siberut strait at this bend (Figure 23b). Second, the 1797 uplift at Badgugu (Bdg) is about twice as large as 1833 uplift there. This hints that uplift of the coasts of Siberut occurred predominantly, and perhaps only, in 1797. Historical reports (Appendix A) also give credibility to the hypothesis that rupture in 1833 did not extend northward beneath Siberut. One account hints that in Padang shaking was more severe in 1797 than in 1833. Tsunami runup at Padang also appears to have been greater in 1797. One account gives a tsunami runup of 3–4 m in Padang in 1833. We estimate from other accounts that runup there was between 5 and 10 m in 1797. Another indication that rupture did not extend beneath Siberut in 1833 is the comparison of tsunami severity in Padang and Bengkulu in 1833; tsunami damage appears to have been greater in Bengkulu and Indrapura (Figure 2) than in Padang. This suggests that the primary source of the tsunami was offshore from Indrapura and Bengkulu, well south of Padang.

[82] In this section we construct models of the 1797 and 1833 ruptures based upon the observed magnitudes and patterns of emergence in 1797 and 1833, adhering to our favored interpretations of the Pitogat and Silogui data (Figures 23b and 24b). As have many earlier investigators [e.g., Kanamori, 1973; Savage, 1983; Thatcher and Rundle, 1984; Zachariassen et al., 1999], we do this by constructing elastic dislocation models that attempt to reproduce the pattern of surface deformation.

[83] A principal constraint in the models is the geometry and location of the megathrust. We fix its position and shape from its outcrop on the seafloor, as defined by bathymetry at the deformation front, and by assuming it is coincident with the top of the Wadati-Benioff zone (based upon locations of hypocenters from the relocated ISC catalogue for the period 1964–1998 [Engdahl et al., 1998]). We also constrain the dislocation to be purely dip slip and choose a dip of 15° , the

Figure 24. Maps of uplift associated with the 1797 earthquake. Uplift ranges as high as about 80 cm, much less than in 1833. The southeastern edge of uplift occurs along the southeastern shores of South Pagai island, and the northwestern edge is in the Batu islands. (a) Contours of uplift assuming nearly equal partitioning of slip between 1797 and 1833 events at Silogui (Slg) and Pitogat (Ptg). (b) Contours of uplift assuming no uplift at Silogui and Pitogat occurred in 1833.

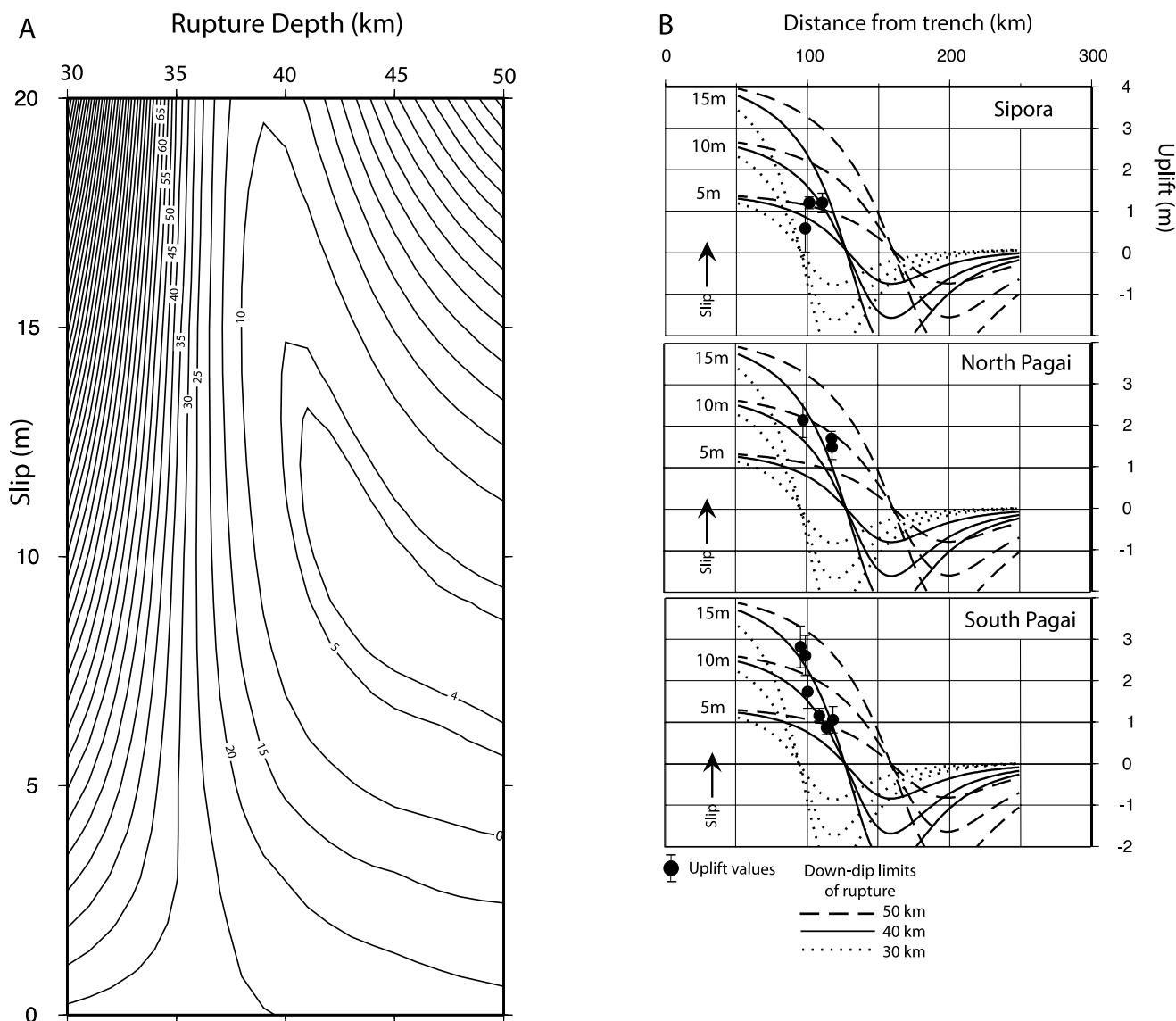


Figure 25. A survey of plausible fits to the uplifts of 1833, in which a rectangular rupture patch with uniform slip extends updip to the trench. (a) The χ^2 values as a function of down-dip rupture limit and slip. Although models with about 7 m of slip and 45- to 50-km down-dip rupture depths fit best, no uniform model fits well. (b) Plots of uplift patterns for transects across Sipora, North Pagai, and South Pagai drawn perpendicular to trench strike display the fits of nine models to data from the coastlines of each island. Each island's data (dots) are fit best with different slip values and down-dip limits of rupture. This warrants a search for composite forward models.

best fitting value for the megathrust beneath the islands. This seems justified, given that instrumentally recorded events in the region overwhelmingly have slip vectors with no more than a small strike-slip component [McCaffrey, 1991].

5.2.1. Elastic Dislocation Models of the 1833 Event

[84] We follow Okada [1992] and start with simple models in which the rupture plane is a rectangular patch, embedded in an elastic half-space beneath the region of uplift and has uniform slip throughout. Figure 25a shows that for megathrust ruptures that extend updip to the seafloor (7 km), best fitting models have slip ranging from about 7 to 10 m and down-dip limits of faulting ranging between depths of about 45 to 50 km. The fact that the χ^2

values are 4 or higher, though, shows that none of these uniform, rectangular models fit the data well.

[85] One way to improve the fit to the data is to subdivide the megathrust beneath the islands into two or more smaller rectangles with differing slip amounts and down-dip limits of rupture. Figure 25b illustrates in three plots a range of fits to the data on Sipora, North Pagai, and South Pagai. In Figure 25b, each plot has nine solutions, permutations of 5, 10, and 15 m of slip with 30-, 40-, and 50-km down-dip depths. Among these nine models, the best fitting for Sipora is the model with 5 m of slip and a locking depth of 50 km. However, for the data from North Pagai island, the best fitting of the nine models is the one with 10 m of slip and a 50-km locking depth. The best fitting of the models for the

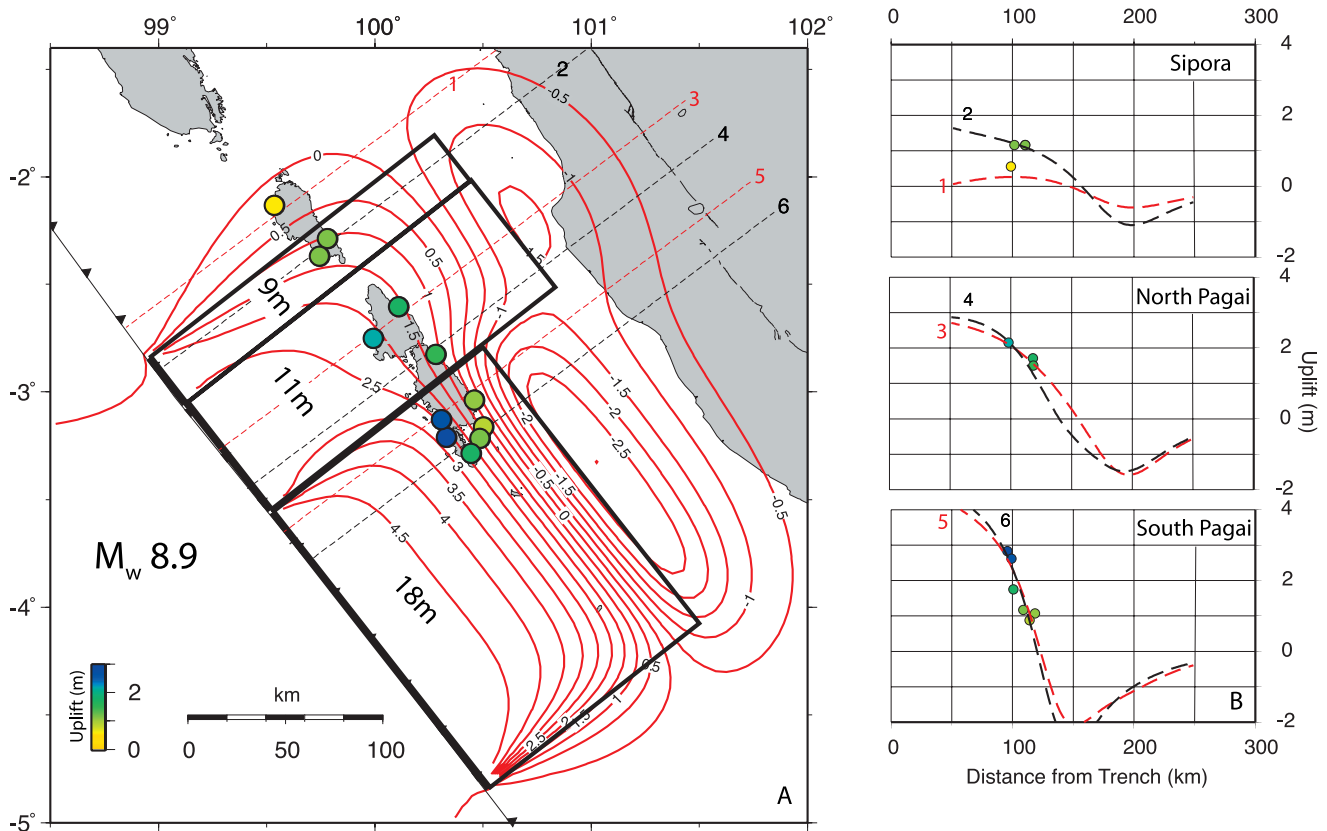


Figure 26. Composite forward models for the 1833 rupture beneath the Mentawai islands. (a) Map view of model in which slip extends updip to the trench. Red contours are modeled uplift and subsidence; colored dots are data. Slip increases from 9 m on the northwestern patch to 18 m on the southeastern patch. Depth of the downdip limit of rupture decreases southeastward from 50 to 37 km. (b) Graph of uplift versus distance from the trench showing separately the fit to the data from Sipora, North Pagai, and South Pagai. (c) Map view of alternative rupture model for the 1833 earthquake, in which the updip limit of faulting is at a depth of 20 km. Slip in this model varies from 7 m in the northwest to 10 m in the southeast. (d) The fit to the data which is not as good as in case of slip extending to the trench. Nonetheless, a comparison of this fit with that in Figure 26b shows that the coral data are insensitive to slip on the megathrust near the trench.

data from the coasts of South Pagai island is the one with 15 m of slip and a downdip locking depth of 40 km.

[86] Guided by these initial tests of best fitting models, we now construct a composite forward model that fits all the data optimally. The model consists of three rectangular patches, one under Sipora, one under North Pagai and one under South Pagai (Figure 26a). The patches under Sipora and North Pagai extend from the trench to a depth of 50 km. Under Sipora, slip is 9 m; under North Pagai it is 11 m. The patch under South Pagai has slip of 18 m and extends to a depth of 37 km. We extend this patch southeast to nearly 5°S, because historical reports (Appendix A) suggest rupture extended at least this far, and because modern seismicity is sparse until that latitude. This composite model fits most of the data well, the shallower slope to the data in the north, the steeper slope in the center, and the very steep slope in the south (Figure 26b). The magnitude, M_w , of this rupture would be 8.9. Its principal characteristics are that slip increases southeastward from about 9 m to about 18 m and that the downdip limit of faulting shallows southeastward from about 50 to 37 km. The χ^2 value of this model,

0.95 shows that the model fits most of the 18 data points well.

[87] An alternative composite model that does not include rupture all the way to the trench may also be acceptable but does not fit the data quite as well. Figures 26c and 26d show the fit of a model in which slip ends updip at 20 km. The downdip limits of faulting are 45, 50, and 39 km from northwest to southeast. Slips on the three patches are 7, 9, and 10 m, from northwest to southeast. The χ^2 value for this model is 1.19, slightly greater than the model in Figures 26a and 26b. Its size is much smaller, equivalent to a M_w 8.6.

[88] Clearly, the coral data do not fully constrain rupture characteristics outboard of the islands. However, they do require that the downdip limit of rupture lies at variable distances between the islands and the mainland.

5.2.2. Elastic Dislocation Models of the 1797 Event

[89] As with the modeling of the 1833 event, a successful model of the 1797 source must replicate well the magnitudes of the uplift and the pattern of tilt, which are summarized here: Uplift ranges from zero to about 80 cm. The low values of uplift in the northwest and southeast limit

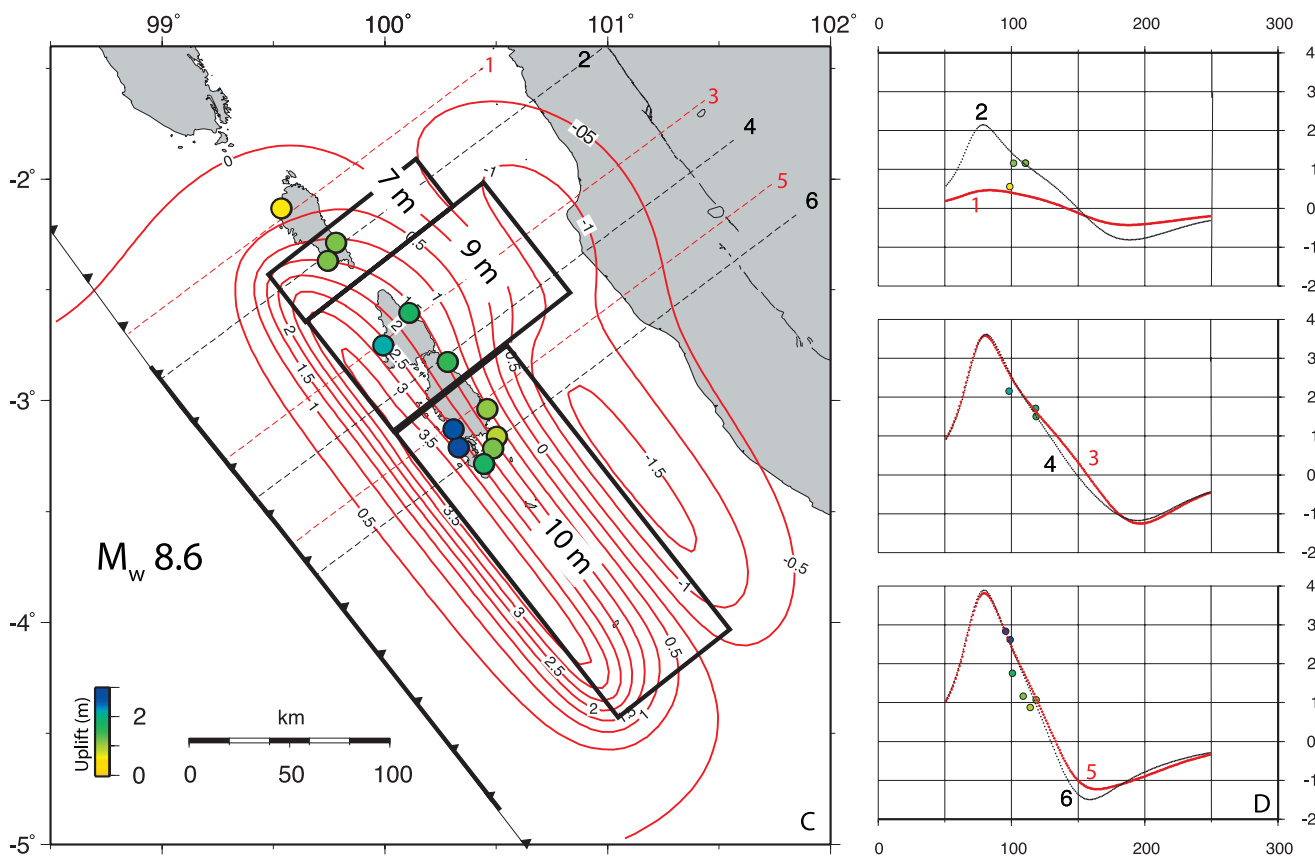


Figure 26. (continued)

the rupture to between about 0.5 and 3.2° S (Figure 24). The southeastern flank of the uplift is remarkably steep, dropping from about 80 cm to zero in less than 20 km. The northeastward tilt of Sipora and North Pagai islands is steep. Also, uplift at one locality on Siberut is no more than about 0.8 m.

[90] As with the 1833 uplifts, we find that there is no simple, uniform slip rupture of the megathrust beneath the Mentawai islands that provides a good fit to the entire data set for 1797. Many points cannot be fit within their errors, as shown by χ^2 values >6 for even the best fitting of the uniform slip rectangular patches. Thus models using combinations of patches are warranted.

[91] For models with rupture out to the trench, one model that fits relatively well is that shown in Figure 27. In this scenario, slip under Siberut is 6 m and extends from the trench to a depth of 40 km. Slip under Sipora is 8 m and the downdip limit of rupture is just 34 km. This shallow downdip limit of rupture yields the steep gradient in uplift that the microatolls record. Under North Pagai and the northern half of South Pagai, slip is 6 m and extends to a depth of 38 km.

[92] No elastic model fits well the steep southeast sloping gradient on southern South Pagai. In this least objectionable model, we use slip of 4 m on a narrow patch with a downdip limit of rupture 50 km. This composite model fits all values except those at the southeasternmost three uplifted sites (Sibelua, Bulasat/Saomang and Singingi). We were unable to fit with an elastic model these three points and the three

points with no uplift farther south (Figure 27). This may indicate that some of the deformation in 1797 was not elastic. Perhaps the half meter underestimation of this model to the uplift documented at Bulasat/Saomang and Sibelua reflects a half meter or so of deformation related to anelastic permanent deformation of the island. Such deformation is shown by outcrops of reef limestone that sit at least 30 m above sea level at the Perak Batu Sumatran GPS Array (SuGAR) station, just a few kilometers north of the Sibelua site (<http://sopac.ucsd.edu/cgi-bin/dbShowArraySitesMap.cgi?site=prkb>).

[93] As in 1833, the emergence and northeastward tilt of all sites on the islands show that the downdip limit of 1797 rupture is northeast of the islands; unlike 1833, however, the downdip limit in 1797 appears to be close to the northeastern coasts of the islands, especially at the latitudes of Sipora and North Pagai. The 1797 displacements are smaller and the 1797 rupture surface is shorter and narrower than those of 1833. Accordingly, the range of magnitudes of the 1797 rupture, M_w 8.5 to 8.7, is appreciably smaller than that of the 1833 rupture. The χ^2 tests show that, taken as a whole, the data are insensitive to the updip limit of rupture. We cannot resolve with these data where the rupture ended between the trench and the southwestern coasts of the islands.

5.3. Postseismic Disturbance at Badgugu

[94] The slight postseismic submergences seen at the northernmost locality, Badgugu, may have an important implication for the 1797 and 1833 events. Badgugu submerged 60 mm after the 1797 event and 140 mm after the

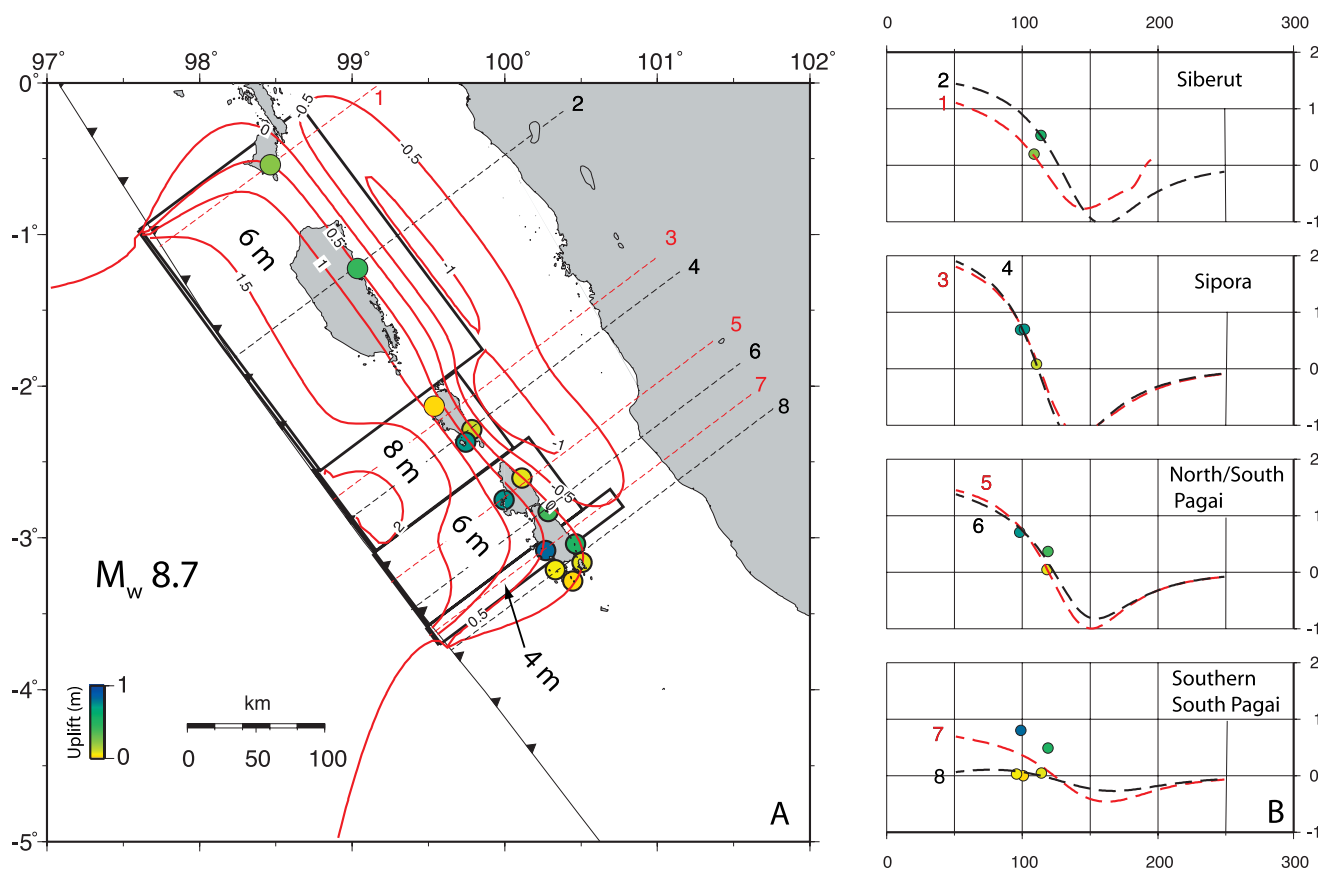


Figure 27. Composite forward model for the 1797 rupture beneath the Mentawai islands, in which slip extends updip to the trench. (a) Map view of the four rectangular patches used to fit the data. Red contours are modeled uplift and subsidence; colored dots are data. Slip varies from 4 to 8 m and the downdip limit of rupture varies between 34 and 45 km. (b) Graphs of uplift versus distance from the trench showing separately the fit to the data from Siberut, Sipora, North Pagai/South Pagai, and southern South Pagai.

1833 event (Figure 22g). In both cases, the postseismic submergence happened in less than 4 years. Because it was greater in 1833 than in 1797, postseismic submergence probably scales with the size of the principal ruptures rather than with the magnitude of slip under Badgugu, which was higher during the lesser of the two earthquakes (1797). This association of greater postseismic submergence with lesser local slip on the megathrust implies a local time-dependent effect related to the overall size of the rupture. One possibility is that these rapid submergences reflect aseismic slip on the megathrust updip from the Badgugu site, as has been shown for postseismic deformation associated with the 2005 giant Nias-Simeulue earthquake [Hsu *et al.*, 2005].

5.4. Paucity of 1797 and 1833 Sites on the Intertidal Reefs Around Siberut

[95] We found only one 18th or 19th century microatoll on the reefs surrounding Siberut island, probably because heads uplifted in 1797 and 1833 having already submerged beneath the intertidal zone there. South of central Sipora ($\sim 2^\circ\text{S}$) fossil heads that died in 1797 or 1833 are readily apparent, because their upper parts protrude 30 to 50 cm above the sea surface during lowest tides. Likewise, north of Siberut, among the Batu islands, the tops of fossil heads that were killed by emergence during the M_w 7.7 earthquake of

1935 protrude into the intertidal zone. Along both of these lengths of the outer arc ridge, then, modern submergence has not exceeded the magnitude of emergence in the most recent large earthquakes.

[96] The scarcity of microatoll sites near Siberut is not due to differences in the reef environment, except perhaps along the vertiginous southwestern coast of the island, where reefs are small, wave energies high and microatolls rare. The character of the eastern coastlines of the Pagai or Batu islands do not differ much from those of northernmost Sipora or Siberut. Furthermore, colonies of living microatolls are abundant along the southern and eastern coasts of Siberut (D. Natawidjaja *et al.*, Intereismic deformation above the Sunda Megathrust recorded in coral microatolls of the Mentawai islands, West Sumatra, submitted to *Journal of Geophysical Research*, 2006). Their pattern of submergence throughout the past half century, in combination with deformations measured with GPS over the past 15 years, indicate that the subjacent part of the megathrust is locked to depths of more than 40 km and stores strain that is released during large earthquakes [Chlieh *et al.*, 2005].

[97] Thus the difficulty in finding 1797 and 1833 vintage microatolls near Siberut must be due to their not protruding into the intertidal zone. The Pitogat and the Silogui micro-

atolls are probably representative; they reside wholly or almost wholly below the modern HLS, that is, below the level of lowest low tides. If these are representative of 18th and 19th century heads from northern Sipora to northernmost Siberut islands, then this readily explains why we were largely unsuccessful in finding more than two.

[98] These findings imply that the emergence on northern Sipora and on Siberut in 1797 and 1833 has been equaled by subsequent submergence. Strictly speaking, though, this is not the case, since sea level has been rising globally 1 to 2 mm/yr for at least the past several decades. Making the generous assumption that this submergence has been occurring for all of the past century, sea level is now 0.1 to 0.2 m above its level in 1797 and 1833. In this case, potential slip on the subjacent megathrust now equals about 80 to 90% of the slip that produced those two giant earthquakes.

5.5. Tsunami Data and Modeling

[99] Historical accounts of both the 1797 and 1833 events include mention of large tsunamis on Sumatran coasts (Appendix A and auxiliary material). One story reports that at some unnamed location the 1797 tsunami surge rose 15 m above normal water level. In Padang, Dutch and German accounts suggest the tsunami surge was at least 5 but less than 10 m deep in 1797 and that inundation extended more than 1 km inland. Historical writings give a less graphic description of the 1833 tsunami in Padang, but one account states that the tsunami surge was 3–4 m high. The extensive destruction of port facilities at Bengkulu suggests that the 1833 tsunami was severe there.

[100] Are these historical tsunami reports compatible with the pattern and magnitude of uplift we have documented and modeled? How do the tsunamis of 1797 and 1833 compare to the Aceh tsunami of 2004? To answer these questions, we modeled the gross features of the tsunamis generated by both earthquake ruptures.

[101] Our simulations employ a linear, dispersive tsunami code [Ward, 2001] and the fault rupture parameters shown in Figures 26a and 27. The waves run over 2-min (~3.7 km) bathymetry from ETOPO2, so tsunami characteristics caused by smaller details are unresolvable and unmodeled. Moreover, the simulation does not carry the waves onto dry land, so the model does not attempt to mimic details of coastal inundation and runup. Rather, wave amplitudes computed directly offshore are scaled to approximate nominal runup amplification as deduced by a range of laboratory experiments on smooth plane beaches. We know that in reality runup can vary over short distances by factors of 2 or 3. Operationally, our runup estimates represent the mean value of a statistical distribution that has a standard deviation roughly equal to the mean. That is, for a quoted runup of say 2 m, perhaps 15% of nearby locations would experience runups >4 m and a few percent of nearby locations would experience runups >6 m.

[102] Like tsunami from all large earthquakes, the model 1797 and 1833 tsunamis beam in directions perpendicular to fault strike. Thus the brunt of the 1797 and 1833 waves run toward the southwest and northeast from their northwest striking sources under the Mentawai islands. Waves traveling into the open Indian Ocean are highest southwest of the sources. Unlike the 2004 Aceh-Andaman tsunami source, which had a nearly north-south orientation (Figure 1), the

1797 and 1833 events do not yield high amplitudes on the coasts of India or Sri Lanka. Because of this tsunami beaming effect and the increasingly east-west trend of the megathrust south of the equator, future earthquakes there probably do not pose a great wave threat to the west coasts of the Bay of Bengal.

[103] The model of the 1833 tsunami indicates that offshore islands shielded mainland locations to the north of the rupture. Note the very slow northwestward progress of nearshore waves (Figure 28). North of Padang, the fastest tsunami waves travel outboard of the islands and then duck in to the mainland coast through the straits between the islands, outpacing the waves propagating through the very shallow waters between the islands and the coast.

[104] The 1833 tsunamis at Meulaboh, Padang and Bengkulu have average runup heights of 1.9, 2.8 and 5.7 m, respectively (Figure 28, left). Among the three mainland coastal localities, Bengkulu, directly east of the 1833 source, receives the strongest waves, consistent with the historical record. Contrast the peak wave heights of 0.4, 0.7, and 2.1 m at three deep-water locations. Each of these is less than the values at the nearby mainland coastal site, because of the amplifications due to shoaling.

[105] The region of uplift in 1797 extended farther north than the uplift of 1833. Modeling of our coral data suggests that 1797 slip averaged about 6 m, about one half to one third the magnitude of slip along the 1833 rupture (Table 3). Generally coseismic uplift, hence tsunami amplitude, scales with slip, so the 1797 tsunami should be far smaller than the 1833 tsunami. Indeed, the 1797 simulation yields lower tsunami amplitudes overall. At Meulaboh, Padang, and Bengkulu the average runups are 1.0, 3.2, and 1.0 m, respectively. For the deep-water sites (Figure 28, traces A, B, and C), the 1797 simulation yields 0.2, 0.85, and 0.1 m. Of the six representative locations, only those closest to the northern part of the 1797 rupture experienced higher values than in 1833. Even so, the modeled 1797 runup of 3.1 m at Padang is only one half to one third the 5- to 10-m wave surge that we infer from the historical record. This difference could be due to a misinterpretation of the historical evidence. Alternatively, details of shallow bathymetry and coastal features near Padang could have pushed wave response beyond the norm. Or, we may have underestimated fault slip for the 1797 earthquake. In regard to the latter, we have only one coral site on Siberut island, so it is possible that uplift was greater in the surrounding waters than what we infer.

[106] To test the modeling with recent observations, we compute tsunami waveforms for the December 2004 event at six representative locations and compare predicted peak wave heights with observed values. For the source of the 2004 tsunami, we use the source parameters given by *Lay et al.* [2005]. Simulation of the 2004 tsunami gives 4.0-, 1.2-, and 1.4-m runups at Meulaboh, Padang and Bengkulu and 1.1, 0.6, and 0.5 m at deep-water sites A, B and C. These calculated runups are lower than observed values. At Meulaboh, the tsunami runup was generally greater than 15 m [*Yalciner et al.*, 2005]. Our interviews of eyewitnesses in Padang harbor indicate that the amplitude of the highest surge there in 2004 was about 2 m (K. Sieh, unpublished field notes, January 2005). Plausible causes for these dis-

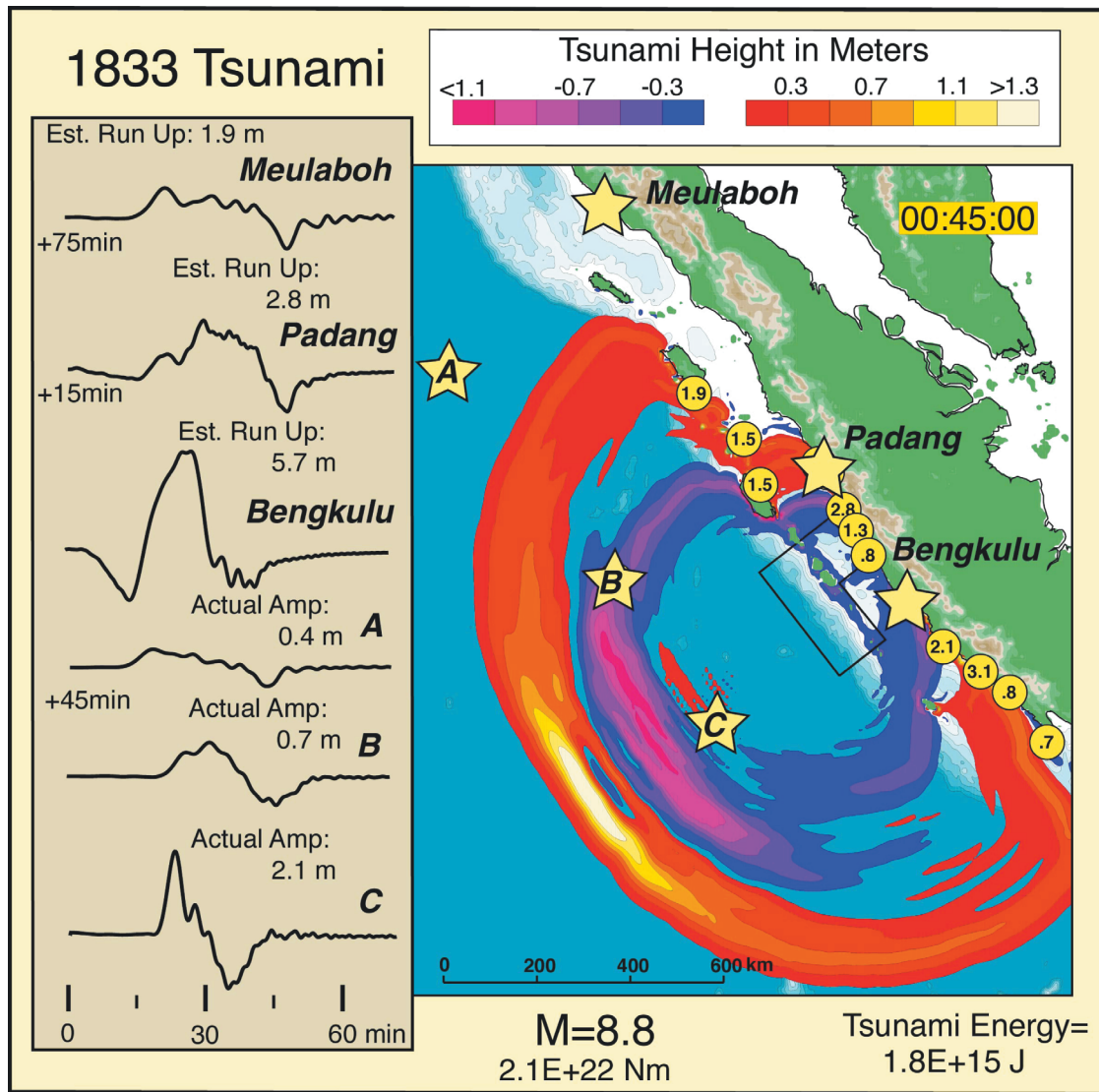


Figure 28. Model of the 1833 tsunami 45 min after the megathrust rupture. Red-to-yellow band shows positive values of the wave; blue-to-red band shows negative values relative to calm sea level. Yellow dots show average runup of tsunami at specific locations along coastlines. Yellow stars show locations of six hypothetical tide gauges, whose tsunami records are on the left. Modeled 1833 average tsunami runup at Bengkulu (5.7 m) is slightly higher than modeled runup of the 2004 tsunami at Meulaboh.

crepancies between model and actual values are the same as in the case of the 1797 model.

[107] Comparison of the 1797, 1833, and 2004 tsunami simulations suggests that great earthquake ruptures offshore Padang and Bengkulu are capable of generating tsunami runups of many meters, similar to those generated along much of the mainland west coast of Aceh in 2004. More detailed analyses will be necessary, however, to assess whether or not the special conditions exist for runups on the Padang-Bengkulu coast to reach the extraordinary 20- to 35-m values experienced at some Aceh localities in 2004.

5.6. Clustering of 1797 and 1833 Events

[108] The interval between the 1797 and 1833 ruptures is much shorter than the average interval between great ruptures of the megathrust there. If all slip occurs seismically, then division of the amount of slip during the earth-

quakes by the convergence rate gives the nominal, average repeat time for the earthquakes. The trench-perpendicular component of convergence across the Sumatran plate boundary is about 45 mm/yr (Figure 1). Slip in the 1797

Table 3. Calculated Tsunami Runup Values at Six Sites for the 1797, 1833, and 2004 Events^a

	1797	1833	2004
A	0.19	0.4	<i>1.1</i>
B	<i>0.85</i>	0.7	0.6
C	0.13	2.1	0.5
Meulaboh	1.03	1.9	4.0
Padang	3.17	2.8	1.2
Bengkulu	0.99	5.7	1.4

^aValues are in meters. Bold values are for coastal sites closest to the tsunami source. Italicized values are for open ocean sites closest to the tsunami source. Refer to Figure 28 for locations.

model averages about 6 m (Figure 27). Hence, if 1797-type earthquakes were periodic and characteristic, they would recur about every 130 years. Likewise, the average slips of about 15 and 10 m in the 1833 models (Figure 26) would correspond to return periods of about 330 years and 220 years. All of these calculations yield intervals that are much longer than the 37 years between the two great earthquakes. These long calculated intervals are consistent, however, with an apparent lack of previous giant earthquakes in the historical record, which extends back to about A.D. 1680 [Newcomb and McCann, 1987].

[109] Furthermore, the amount of slip that occurred beneath the islands in 1833 is far greater than could have accumulated between 1797 and 1833. Beneath Sipora and North Pagai, model slip in 1833 is about 10 m. If all of this had accumulated in just 37 years, the rate of trench-perpendicular convergence would have been about 270 mm/yr, which is many times greater than the known rate.

[110] Both of these observations imply that the 1797 and 1833 ruptures comprise a couplet that relieved strains that had accumulated in prior centuries. Slip in 1797 did not relieve all strains that had occurred in the previous interseismic period, and slip in 1833 relieved more than just those strains that had accumulated in the years since 1797.

[111] There are at least two other examples of great earthquake couplets. Paleoseismic and historical records [Sieh, 1984; Jacoby et al., 1988; Sieh et al., 1989; Weldon et al., 2004] show that the great 1812 and 1857 ruptures of the Mojave section of the San Andreas fault were preceded by about 300 years of dormancy. Slip during both events was about 6 m. The 6 m of slip that occurred in 1812 would account for about half of the strain accumulated at about 35 mm/yr in the prior three centuries. Taken together, however, these two slips plausibly accounts for all of the strain that had accumulated in the preceding three centuries. Recent ruptures of the dextral strike-slip Denali fault provide another example. At the crossing of the Trans-Alaska pipeline, slip during the great M_w 7.9 earthquake of 2002 was about 5 m [Eberhart-Phillips et al., 2003]. At the 10 mm/yr average slip rate of the fault at this location [Meriaux et al., 2004], an average recurrence interval for such ruptures would be about 500 years. Nonetheless, a rupture large enough to severely disturb trees along the fault occurred just 90 years earlier, in 1912 [Carver et al., 2004]. It is highly unlikely that the strains necessary to result in a 5-m right-lateral slip could have accumulated in the 90 years between 1912 and 2002.

[112] These three examples of great rupture couplets demonstrate that some large fault ruptures do not relieve all or even most of the elastic strains that had accumulated prior to their occurrence. Rather than ushering in a long period of dormancy, the first event in the couplet is followed within decades by an even larger rupture. In the case of both the 1812 San Andreas and Mentawai 1797 events, and perhaps in the case of the 1912 Denali event as well, the rupture relieved appreciably less elastic strain than had been accumulated through the long antecedent period of dormancy. This could have been a warning that the second event was in the offing.

[113] Given the existence of the 1797 and 1833 couplet, one should ask whether or not the recent great Aceh-Andaman and Nias-Simeulue earthquakes of 2004 and

2005 could each also represent the first in a couplet. The correct answers are uncertain, because the date and nature of previous great ruptures along those two sections of the megathrust are poorly known. The megathrust beneath Nias island has the best constraints. Rupture under Nias during the 2005 Nias-Simeulue event averaged about 6 m [Briggs et al., 2006]. At the rate of strain accumulation (Figure 29), strains leading to this amount of slip would accrue in about 140 years. Since this is almost precisely the time between 2005 and the previous great earthquake in 1861, it is unlikely that a re-rupture of the megathrust under Nias will happen in the next few decades. The history of the northern half of the 2005 rupture is too poorly known to forecast its behavior over the next few decades. Likewise, the history of the megathrust along the 1600-km-long rupture of 2004 is too poorly known to venture a strong opinion.

5.7. Scenarios for Future Events

[114] Four observations are relevant with respect to the future behavior of the Sunda megathrust in the region of the great 1797 and 1833 earthquakes and tsunamis. First, between about 0.5°S and the equator, it appears that the megathrust does not, for the most part, participate in the generation of great earthquakes. Coral records show that the 1797 and 1833 ruptures halted at the southern edge of this section (Figure 29). Furthermore, the great ruptures of 1861 and 2005 ended near the northern limit [Newcomb and McCann, 1987; Briggs et al., 2006] (Figure 22a). The largest sudden rupture of this part of the megathrust in the past 250 years is a 2.3-m slippage during the M_w 7.7 earthquake of 1935 [Natawidjaja et al., 2004]. Thus this part of the megathrust is likely a northern barrier to rupture under the Mentawais.

[115] Second, the microatolls of Siberut island that emerged in 1797 and possibly 1833 are now at or below the tops of modern living microatolls. This indicates that submergence over the past two centuries has nearly compensated for emergence during those events. If this were not true, we would have found an abundance of 1797/1833 microatolls above water during low tides. In contrast, at all our sites south of about 2°S, 1833 microatolls still protrude above the lowest low tides, generally by a few hundred millimeters. This indicates that strain accumulation since 1833 has not compensated for emergence during that event. A similar conclusion can be drawn for the Batu islands, where heads that emerged in 1935 still reside well above their levels just before that earthquake.

[116] Thus the deficit of strain relief at the latitude of Siberut is greater than to the southeast or northwest, normalized to the size of the previous rupture. One can imagine scenarios for a future megathrust earthquake in which the 150-km-long Siberut section fails separately. However, since faults do not always recoup all the strain relieved by a previous earthquake prior to generating another, it is also possible that the Siberut and northern Sipora sections will fail in concert with the next rupture of the sections that failed in 1833.

[117] A third pertinent observation is that modern seismicity roughly outlines the sides and downdip edges of the 1797 and 1833 ruptures (Figure 29). Since background seismicity commonly is sparse on a locked patch [e.g., Subarya et al., 2006], the 1797 and 1833 downdip limits

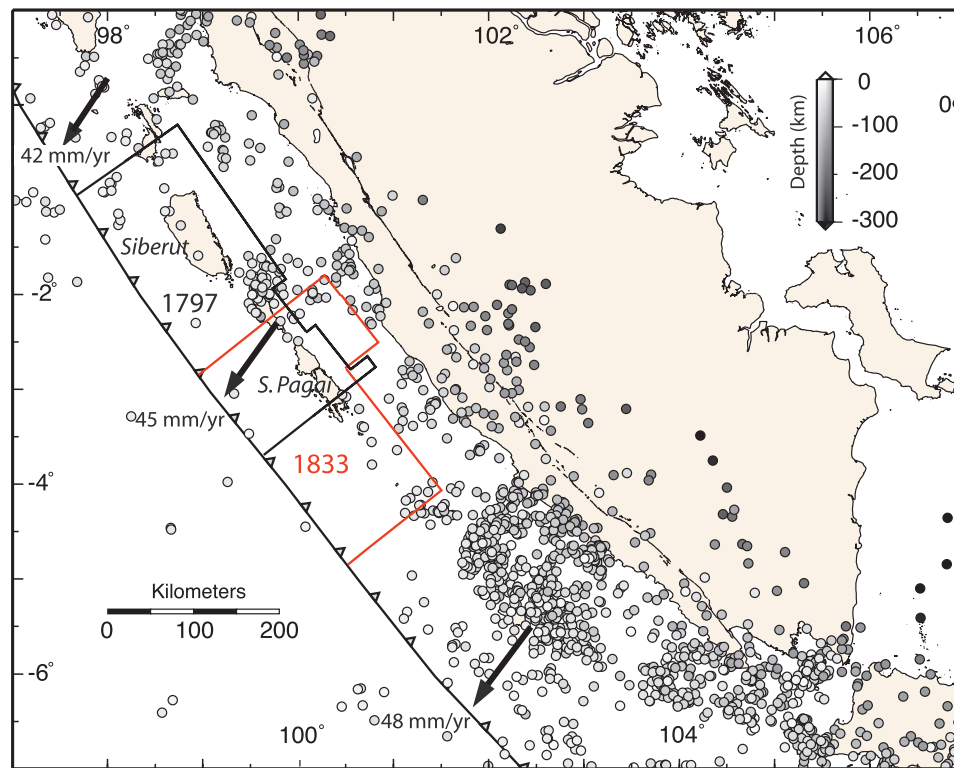


Figure 29. Map of the 1797 and 1833 rupture planes and modern seismicity showing that modern seismicity is low in the region of the great ruptures but high in the surrounding regions. This suggests that the modern locked patch is similar in dimension to the patches that broke in 1797 and 1833. Epicenters are from the Harvard CMT catalog for the period 1977 to 2005 (<http://www.seismology.harvard.edu/CMTsearch.html>).

likely approximate the downdip limits of future ruptures as well. This locked Mentawai patch has a cluster of recent earthquakes between Sipora and Siberut islands. The most recent flurry of earthquakes there were aftershocks that occurred two weeks after the March 2005 Nias-Simeulue M_w 8.7 earthquake (http://neic.usgs.gov/neis/eqlists/sig_2005.html). This location coincides with a major change in the character of the 1833 rupture and the crossover between compensated and overcompensated 1797 and 1833 microatoll populations. High concentrations of stress at this change in 1833 rupture behavior could have made this area unusually sensitive to additional loading by the Nias-Simeulue rupture of 2005.

[118] The fourth observation relevant to forecasting future ruptures of the locked Mentawai patch concerns the section of the megathrust along the southernmost Sumatran coast, between Enganno island and the Sunda Strait (Figure 1). No one has proposed that the 1833 rupture extended into this region. Is this 300-km-long section capable of rupturing during a great earthquake? Or is it like the Javan section of the megathrust to the east, alleged to be weakly coupled and capable of generating only moderate to major quakes?

6. Summary and Conclusions

[119] Records of vertical deformation contained in fossil and modern coral microatolls reveal uplift associated with the great Sumatran earthquake of 1833 (Figure 23). The

corals show that along at least a 170-km span of the Sumatran outer arc ridge, uplift ranged between 1 and 3 m, with pronounced tilts toward the mainland, as occurred during the great rupture of the Sunda megathrust in 2005 [Briggs *et al.*, 2006]. Elastic-dislocation modeling of these data yield a preferred forward model characterized by a southeastward increase in slip from 9 to 18 m and a southeastward decrease in the downdip limit of rupture from 50 km to 37 km (Figure 26a). Our data do not allow us to resolve the updip limit of rupture; models with updip limits at 20 km depth (Figure 26c) fit the data nearly as well as our favored model, in which rupture extends all the way to the trench. The pattern of uplift indicates that rupture continued southeast from the Mentawai islands, consistent with the inference from historical accounts that the rupture extended an additional 220 km or so to the southeast. The northwestern limit of rupture is likely at about 2°S, but may have extended as much as 160 km farther northwest with much smaller amounts of slip. The earthquake magnitudes indicated by the range of plausible rupture parameters range from M_w 8.7–8.9.

[120] The coral records demonstrate that significant uplift of the outer arc islands also occurred 37 years earlier, in 1797 (Figure 24). As in 1833, the islands tilted toward the mainland, but uplift amounts were a factor of 2–3 smaller where the ruptures overlap. The southeastern limit of uplift in the 1797 event occurs on South Pagai island, so the southeastern limit of rupture is well constrained to about

3.2°S. Our forward models of the 1797 megathrust rupture have rupture lengths of at least 160 km under the islands. The 1797 rupture likely extended northwest 160 km beyond the 1833 rupture, terminating at a section of the megathrust that slips primarily aseismically, near 0.5°S. Our favored model has a 360-km-long source that consists of four rectangular patches with slips of 4 to 8 m and with downdip limits of rupture that range from 34 to 50 km. We obtain a magnitude of 8.5 for the model with a 20-km-deep updip rupture limit and an 8.7 for the case of the megathrust breaking to the seafloor.

[121] The modeled downdip limits of the 1797 and 1833 ruptures are similar to the current downdip limit of the currently locked patch, as judged from background seismicity.

[122] History records that both the 1797 and 1833 earthquakes generated large, destructive tsunamis (Appendix A). Both the shaking and tsunami runup appears from these accounts to have been more severe in 1797 at Padang, opposite Siberut. This supports our microatoll-based conclusion that the 1797 rupture, though smaller, extended closer to Padang than the 1833 rupture. Our simulations of the 1797 and 1833 tsunamis on the mainland coast yield runup values consistent with historical accounts. Whether values were locally as high as the 20- to 35-m values seen in Aceh in 2004 cannot be resolved without more detailed modeling or observation. However, it is clear from our modeling of the 1797 and 1833 tsunamis that rupture of the megathrust south of the equator should not be expected to produce large tsunamis along the western coasts of the Bay of Bengal.

[123] A significant improvement in our initial assessments of the source parameters of the 1797 and 1833 earthquakes could result from additional work. Certainly there are other microatoll sites along the outer arc ridge that remain to be sampled. In particular, data from the islands along strike to the southeast, between 3.5° and 5.5°S, could help constrain the magnitude and limits of the 1833 rupture. A more thorough search for vintage 18th and 19th century microatolls beneath lowest low tides on the fringing reefs of Siberut island would constrain the ruptures of 1797 and 1833 much better there.

[124] Moreover, paleoseismic work in the marshes and estuaries of the mainland coast would likely yield important results. On the mainland coast, it may be possible to recover records of submergence and tsunamis associated with a series of late Holocene megathrust ruptures, as at the Cascadia subduction zone and in south central Chile [Atwater *et al.*, 2004]. The absence or presence of submergence during the 18th and 19th centuries would provide constraints on the northwestern extent of rupture that are more compelling. Such work might also constrain better the downdip limits of rupture and the magnitude of slip in both events. These investigations would likely also yield minimum tsunami inundation distances.

[125] Similar investigations along the southernmost Sumatran coast could support or refute the hypothesis that southward of 5.5°S and along the coast of Java the megathrust is incapable of producing great earthquakes [Newcomb and McCann, 1987].

[126] Finally, a more thorough search of historical records would likely add substantially to knowledge of the levels of shaking and size of the 1797 and 1833 tsunamis.

Appendix A: Historical Accounts of the 1797 and 1833 Earthquakes and Tsunamis

[127] In the course of our work on the 1797 and 1833 earthquakes, we have come across several written accounts of the earthquakes and tsunamis, of which this appendix is an interpretive summary. To make the full text of the accounts readily accessible, we provide them as auxiliary material (Text S1). Below, we summarize these historical accounts. Figure 1 shows the locations of most places mentioned in the accounts. The settlement of Padang is depicted in Figure A1, as it was in 1781 and 1828 (Figures A1a and A1b). The southernmost part of the modern city, nearest the old settlement, is shown in Figure A1c, for comparison.

A1. The 1797 (10 February, About 2200 LT) Earthquake

A1.1. Summary

[128] All reports of this earthquake are from Padang or nearby. They indicate that the 1797 earthquake caused considerable damage in Padang, but that only two lives were lost there. Tsunami surges caused damage in Padang and deaths in Air Manis (Figure A1) and affected the Batu islands.

A1.2. The Shaking

[129] The duration of the shaking in Padang was one minute. A report published in 1845 [du Puy, 1845] indicates that it was the strongest earthquake in the memory of residents of Padang. By contrast, a report published in 1847 [du Puy, 1847] states that at the time of the 1797 event older people recalled that a stronger earthquake had occurred 40 years prior to 1797. Many houses collapsed or were severely damaged and 3 to 4 inch fissures appeared in the ground.

A1.3. The Tsunami

[130] Several people who climbed trees to escape the tsunami at Air Manis were found the next day, dead in the branches. That whole town was flooded and several houses washed away. The tsunami at Padang also flooded the “whole place” and consisted of three or four ebbs and surges in the river harbor. One report indicates that the surge rose one third the height of the Apenberg, the 104-m-high peninsula that juts out from the south bank of the river (i.e., about 34 m). That report states that the peninsula “broke the force of the tsunami somewhat.” Another report states that during the tsunami the water level rose (at an unnamed location) 50 feet above normal. At Padang, the ebbs left the riverbed dry and the surges left fish on the riverbanks. All the boats in the river ended up on dry land. A 150- to 200-t English sailing ship that was tied to a tree near the mouth of the harbor rode the surge 0.75 English miles up river (to behind either the fort or the bird market, depending on the account), destroying three homes while in transit. The surges carried several smaller boats up the river as well and deposited them behind the market, about 1.8 km from the river mouth. All seaside homes were reported flooded as well.

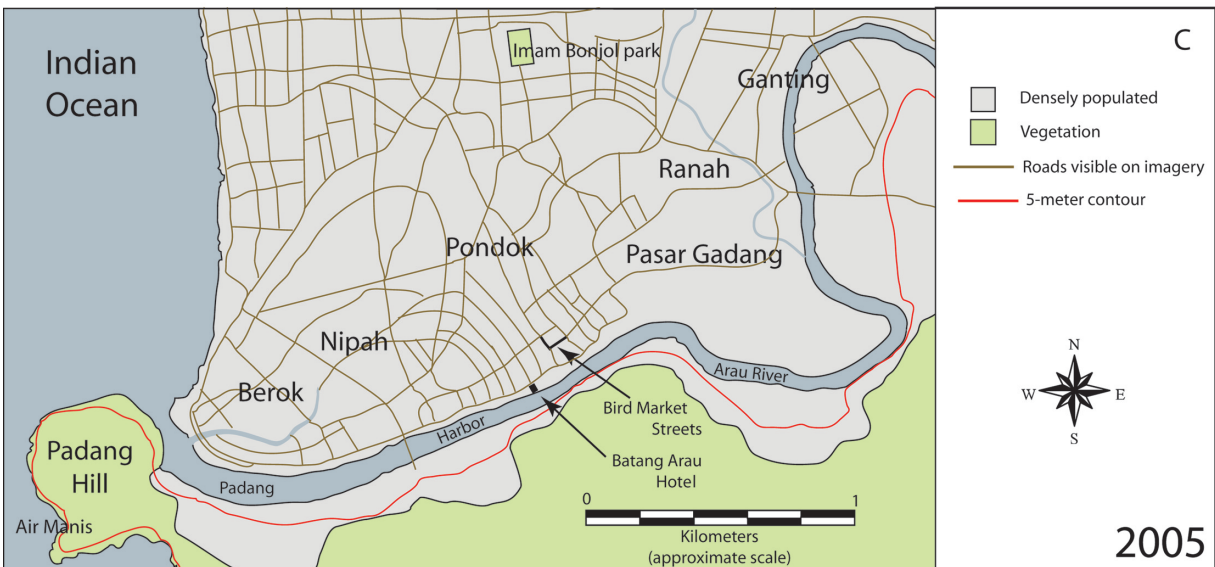
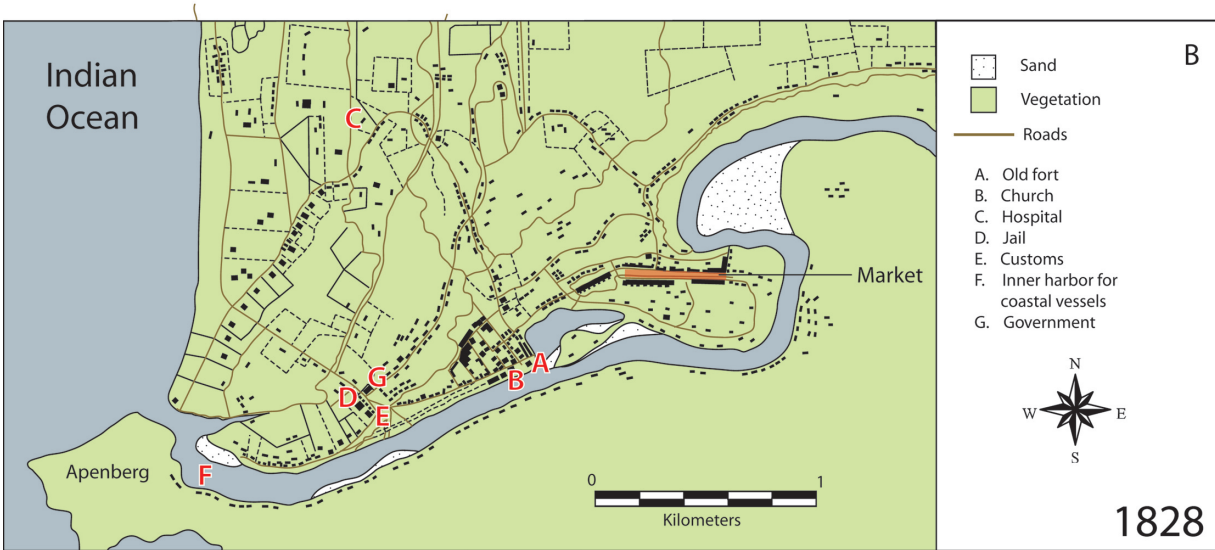
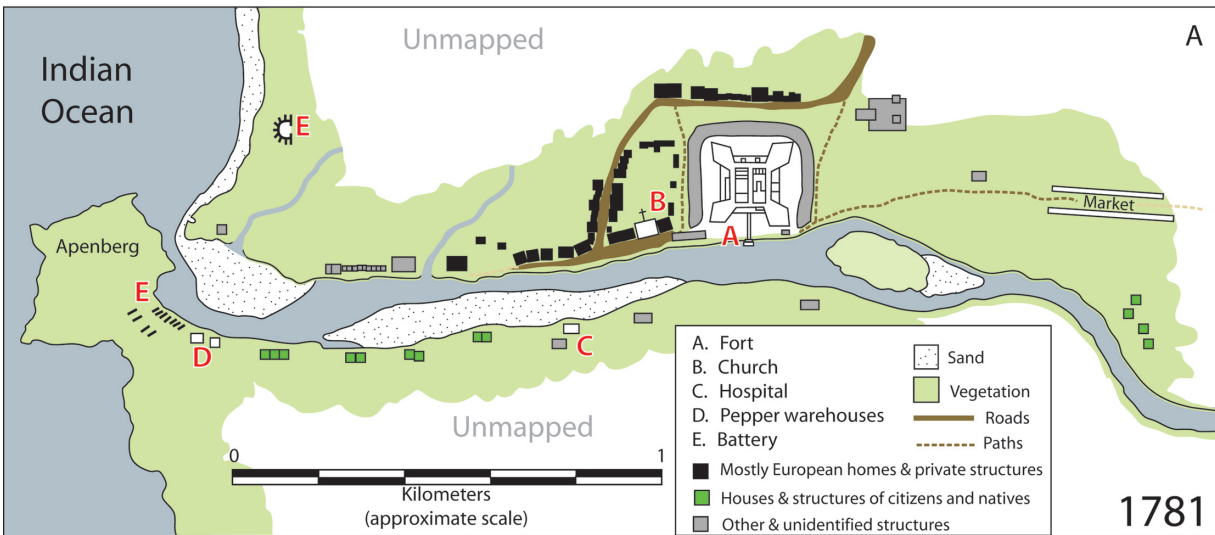


Figure A1

A1.4. Interpretation

[131] The reports of the 1797 earthquake and tsunami focus on tsunami effects near the river, which extends landward from the coast as Padang's harbor. This probably should not be taken as an indication that the tsunami inundation was most notable along the river, because the settlement at that time was confined to riverbanks upstream from the coast (Figure A1). At Air Manis, a small village on the exposed western side of the Apenberg, the tsunami rose high enough to drown people who had climbed trees to escape the tsunami. The trees would probably have to have been at least 4 or 5 m tall to support the weight of an adult Indonesian, so this seems to constrain the minimum flow depth of the tsunami there. The grounding of the English ship behind the fort or bird market suggests a flow depth at least this high. The current riverbank walls are about 2 m high, and the draft of the ship was probably at least 3 m. Thus it is reasonable to believe the tsunami runup was at least 5 m. This is still far less than the purported ~30-m runup on the flank of the Apenberg, which juts out from the harbor and the reported 50-foot (15-m) runup elsewhere along the coast. It is doubtful that the tsunami flow depth could have been as high as 15 or 30 m at Padang, for surely this would have caused the wholesale destruction of the settlement and a far greater loss of life. We suggest that a flow depth of between 5 and 10 m at Padang is most consistent with the available historical data.

A2. The 1833 (24 November, About 2000 LT) Earthquake

A2.1. Summary

[132] The earthquake lasted 5 minutes at Bengkulu and about 3 minutes at Padang. It was felt as far away as Singapore and Java. Damaging tsunamis occurred at Bengkulu, Pulau Cinco, Indrapurah, Padang, and Pariaman. Reports say that no one died in Bengkulu and only one native died in Padang.

A2.2. The Shaking

[133] Shaking was severe along the coast from Bengkulu to Pariaman and at sea near the Pagai islands. In Pariaman the shaking was so strong that no one could stand. Damage was substantial in both Padang and Bengkulu, but was greater in Bengkulu, where all structures were damaged and the fort and tower had to be torn down. In Padang, wooden houses fared well but many stone structures lost walls and roofs. Huts collapsed as far away as Palembang, in eastern Sumatra. Fissures a couple feet wide occurred in

Pariaman, and fissures formed in the beach between Pariaman and Padang and along the riverbank in Padang.

A2.3. The Tsunami

[134] In Padang, ships moved on their anchors and some were lost. The sea ran up 3–4 m at the beach. The map of 1828 (Figure A1b) shows sparse settlement along the beach and the center of town still along the northern bank of the river, a kilometer or more inland. The pier and customs building at Bengkulu were wiped out, and some boats were deposited upon the beach. In Pariaman, the tsunami started with the withdrawal of the sea. The surge tore all boats from their anchors and carried them “to the left and right.” At Pulau Cinco (~100 km southeast of Padang, near the mainland coast) the sea rushed in and carried away several houses and people. At Indrapura, “terrible waves” rolled in over the low countryside and one village was completely washed away. One woman and her child were swept away, but many people survived by climbing trees and waiting there until morning. In the Seychelles, 5000 km west of Sumatra in the Indian Ocean, the 1833 tsunami was similar to that which followed the giant Aceh-Andaman earthquake of 2004.

A2.4. Volcanic Phenomena

[135] Two volcanoes, Marapi and Kerinci showed heightened activity after the earthquake. Collapse of a natural dam high on Kaba volcano led to flooding of the valleys to the southeast of the volcano, with the loss of 90 people in two districts. One village was flooded to a depth of 20 feet and was left buried in 7 feet of mud.

A2.5. Interpretation

[136] The long duration of the earthquake and its severity certainly suggest a very large source rupture. The clear indication that the earthquake was more severe at Bengkulu than at Padang may indicate that the rupture extended well south of the Pagai islands and that it did not extend as far north as Padang. The description of the earthquake at Padang as “oscillatory” could be construed to mean that short-period motions were less pronounced than sensible long-period motions. Tsunami damage appears to have been greater at Indrapura and Bengkulu than at Padang. Boats were torn from their moorings in Pariaman and Padang, but the descriptions imply (but do not expressly state) that the water did not surge over the riverbanks as it had in 1797. Nonetheless, the surge rose 3–4 m at the beach in Padang, which would have been high enough to flood at least a few hundred meters inland, given that the earthquake occurred during a spring tide and that elevations are under 5 m up to at least a kilometer inland. This might not have inundated

Figure A1. Maps of Padang that include locations mentioned in historical accounts of the 1797 and 1833 earthquakes and tsunamis. (a) Padang in 1781, which was a small settlement of a few dozen private and government structures about a kilometer from the sea. Reports indicate that the 1797 tsunami carried a large English ship from its anchorage near the river mouth to the part of the town north of the Fort called the Bird Market. The tsunami also carried smaller boats to the large market, east of the main town. Adapted from *Netscher* [1881]. (b) Padang in 1828, which was a larger settlement but still concentrated upstream from the river mouth. The tsunami surge in 1833 is reported to have been 3–4 m high at the coast. Adapted from *de Stuers* [1849]. (c) Map of the modern city of Padang showing that dense settlement extends from the shoreline landward for more than 3 km and is mostly less than 5 m above sea level. Bird Market Streets may mark the location of the bird market, where the English ship was deposited by the tsunami surge in 1797. The 2005 map is drafted from satellite imagery. Location of Bird Market Streets and Batang Arau Hotel are constrained by handheld GPS determinations.

many structures, given the sparse settlement near the beach shown on the 1828 map (Figure A1).

Appendix B: Explanation of the Growth of Coral Microatolls Relative to Sea Level

[137] Although previous papers describe the use of a coral microatoll to measure changes in sea level [e.g., Zachariassen *et al.*, 1999, 2000; Natawidjaja *et al.*, 2004], this appendix offers a reiteration of these earlier explanations, for the convenience of readers of this paper. In addition, two animations of coral growth that help visualize a coral's response to sea level changes are available at <http://es.ucsc.edu/~ward/>.

[138] Massive coral heads such as those used in this study are colonies of individual corallites, one to a few millimeters in diameter, which live on the perimeter of the head. Each corallite produces an aragonitic skeleton that is progressively left behind by the organism as it divides by mitosis and grows radially outward at rates of about 10 mm yr^{-1} . Growth at about this rate produces a coral head with a diameter of about 4 m in 200 years.

[139] When the original organism first attaches itself to the sandy or rocky substrate (Figure B1a, point A), it is some distance below sea level. As the colony grows laterally it becomes more massive and develops a broader base, qualities that give it stability in the nearshore environment. The vertical growth of the colony eventually brings its uppermost living corallites to the level of lowest low tides (Figure B1, level b). These uppermost corallites do not survive long out of the water. *Porites* corallites of the types we use cannot survive at levels greater than about 40 mm above lowest low tide [Briggs *et al.*, 2006]. This uppermost limit to coral growth is called the HLS, an acronym for the highest level of survival [Taylor *et al.*, 1987].

[140] Lateral growth continues below lowest low tide level, but vertical growth is halted at the HLS. If lowest tide levels do not vary over several years, the head develops a flat upper surface (B to C). If sea level suddenly drops, say because of uplift of the reef during an earthquake, the HLS drops the same amount, leaving a dead band of corallites around the perimeter of the head. The difference in elevation between the old HLS and the new one is a measure of the amount of uplift.

[141] In the case of the microatoll in Figure B1, sea level is stable at the new level for 5 years, until growth reaches point D, at which time submergence occurs, either instantaneously or at a rate greater than the corallites can grow upward. The microatoll takes 4 years to reach the new HLS level (E). HLS stays at that level for just a year and then drops again, to level F. Subsequent to that drop, sea level rises rapidly and is tracked by HLS for 10 years, to G. Later periods of rapid subsidence and sea level stability bring the microatoll to its final configuration in Figure B1, at point I and HLS level h. An emergence of about 120 mm kills the entire microatoll at this final stage.

[142] In Figure B1, the top of truncated annual bands are unconformities that represent death of corallites. These unconformities are the features that allow determination of relative sea level history during the life of the microatoll. They are depicted as dots in the graph of HLS history in Figure B1b and in similar figures in the paper. The tops of

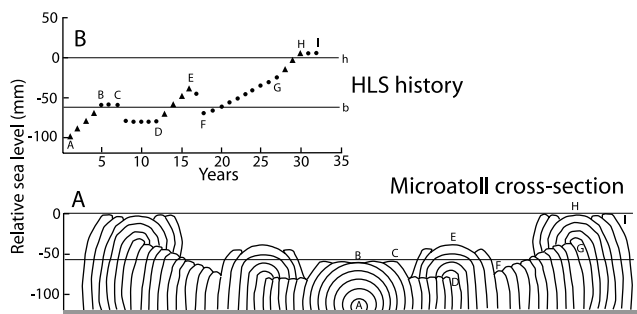


Figure B1. Response of an idealized coral microatoll to changes in sea level. (a) Vertical cross section of the microatoll showing growth of annual bands from A to I. Changes in sea level several times in the 32-yearlong period lead to changes in pattern of growth. (b) Graph of sea level versus time showing years when growth unconformities record lowest annual low tide level (dots) and years when level of highest corallites provide only a minimum constraint (triangles). The highest level of survival of the corals (HLS) is actually a few centimeters higher than lowest low tide.

annual bands that are growing below HLS appear as triangles in the graphs of HLS history.

[143] **Acknowledgments.** Many friends, colleagues, and family provided critical support of our field efforts in 1999, 2000, 2002, and 2003, particularly Imam Suprihanto, Susi Mardia, and Dudi Prayudi. Maarten Schmidt translated historical Dutch accounts of the earthquakes and tsunamis, and Juniator Tulus found many of them. Jenny Briggs translated the German accounts. Historian Jeffrey Hadler helped us find and interpret historical information. Thorough, thoughtful reviews by Brian Atwater and Harvey Kelsey helped us clarify many points and correct mistakes in the manuscript. Carrie Sieh helped improve the figures. Finally, we are greatly indebted to the many people of mainland West Sumatra and the Mentawai islands for their hospitality and friendship. This research was supported by NSF grants EAR-9628301, EAR-9804732, and EAR-9903301 (to K.S.); EAR-9628716, EAR-9903443, and EAR-0207686 (to R.L.E.); and EAR-9804970 (to S.N.W.) and by the Indonesian International Joint Research Program (RUTI). This is contribution 15 of the Tectonics Observatory, California Institute of Technology.

References

- Abercrombie, R. E., M. Antolik, and G. Ekstrom (2003), The June 2000 M_w 7.9 earthquakes south of Sumatra: Deformation in the India-Australia Plate, *J. Geophys. Res.*, *108*(B1), 2018, doi:10.1029/2001JB000674.
- Allen, C. (1968), The tectonic environments of seismically active and inactive areas along the San Andreas fault system, in *Proceedings of Conference on Geologic Problems of San Andreas Fault System*, edited by W. R. Dickinson and A. Grantz, *Stanford Univ. Publ. Geol. Sci.*, *11*, 70–80.
- Atwater, B., M. Tuttle, E. Schweig, C. Rubin, P. Yamaguchi, and E. Hemphill-Haley (2004), Earthquake recurrence inferred from paleoseismology, in *Quaternary Period in the United States*, *Dev. Quat. Sci.*, *1*, edited by A. R. Gillespie, S. C. Porter, and B. F. Atwater, pp. 331–350, Elsevier, New York.
- Bock, Y., L. Prawirodirdjo, J. F. Genrich, C. W. Stevens, R. McCaffrey, C. Subarya, S. S. O. Puntodewo, and E. Calais (2003), Crustal motion in Indonesia from Global Positioning System measurements, *J. Geophys. Res.*, *108*(B8), 2367, doi:10.1029/2001JB000324.
- Boelhouwer, J. C. (1841), *Herinneringen van mijn verblijf op Sumatra's westkust gedurende de jaren, 1831–1834*, Gravenhage: Doorman, The Hague.
- Briggs, R., et al. (2006), Deformation and slip along the Sunda megathrust in the great 2005 Nias-Simeulue earthquake, *Science*, *311*, 1897–1901, doi:10.1126/science.1122602.
- Carver, G., G. Plafker, M. Metz, L. Cluff, B. Slemmons, E. Johnson, J. Roddick, and S. Sorensen (2004), Surface rupture on the Denali fault interpreted from tree damage during the 1912 Delta River M_w 7.2–7.4 earthquake: Implications for the 2002 Denali fault earthquake slip distribution., *Bull. Seismol. Soc. Am.*, *94*, S58–S71.

- Cheng, H., J. Adkins, R. Edwards, and E. Boyle (2000), U-Th dating of deep-sea corals, *Geochim. Cosmochim. Acta*, 64(14), 2401–2416, doi:10.1016/S0016-7037(99)00422-6.
- Chhibber, H. (1934), *Geology of Burma*, 538 pp., McMillan, London.
- Chlieh, M., et al. (2005), Coseismic slip and afterslip associated to the M_w 9.14 Aceh-Andaman earthquake, *Eos Trans. AGU*, 86(52), Fall Meet. Suppl., Abstract U21C-01.
- Church, J., and N. White (2006), A 20th century acceleration in global sea-level rise, *Geophys. Res. Lett.*, 33, L01602, doi:10.1029/2005GL024826.
- Cobb, K. M., C. Charles, H. Cheng, M. Kastner, and R. Edwards (2003), U/Th-dating living and young fossil corals from the central tropical Pacific, *Earth Planet. Sci. Lett.*, 210(1–2), 91–103, doi:10.1016/S0012-821X(03)00138-9.
- Darwin, C. (1842), *The Structure and Distribution of Coral Reefs*, 278 pp., Smith, Elder, London.
- Deplus, C., M. Diamant, H. Hébert, J. Dubois, P. Patriat, J. Sibilla, G. Bertrand, S. Dominguez, J. Malod, and B. Pontoise (1998), Direct evidence of active deformation in the eastern Indian oceanic plate, *Geology*, 26(2), 131–134, doi:10.1130/0091-7613.
- DeShon, H. R., E. R. Engdahl, C. H. Thurber, and M. Brudzinski (2005), Constraining the boundary between the Sunda and Andaman subduction systems: Evidence from the 2002 M_w 7.3 northern Sumatra earthquake and aftershock relocations of the 2004 and 2005 great earthquakes, *Geophys. Res. Lett.*, 32, L24307, doi:10.1029/2005GL024188.
- de Stuers, H., (1849) De Vestiging en Uitbreiding der Nederlanders ter Westkust van Sumatra, vol. 1, 239 pp., P. N. van Kampen, Amsterdam.
- du Puy, J. (1845), Een aantekening omtrent vuurbergen en aardbevingen op Sumatra, *Tijdsch. Neerland's Indie*, 7.
- du Puy, J. (1847), Een paar aantekeningen omtrent vuurbergen en aardbevingen op Sumatra, *Tijdsch. Neerland's Indie*, 9.
- Eberhart-Phillips, D., et al. (2003), The 2002 Denali Fault earthquake, Alaska: A large magnitude, slip-partitioned event, *Science*, 300, 1113–1118.
- Edwards, R. L., J. Chen, T. Ku, and G. Wasserburg (1987), Precise timing of the last interglacial period from mass spectrometric determination of ^{230}Th in corals, *Science*, 236, 1547–1553.
- Edwards, R. L., F. Taylor, and G. Wasserburg (1988), Dating earthquakes with high-precision thorium-230 ages of very young corals, *Earth Planet. Sci. Lett.*, 90(4), 371–381.
- Engdahl, E. R., van der Hilst, and R. Buland (1998), Global teleseismic earthquake relocation with improved travel times and procedures for depth determination, *Seismol. Soc. Am. Bull.*, 88(3), 722–743.
- Fitch, T. (1972), Plate convergence, transcurrent faults, and internal deformation adjacent to Southeast Asia and the western Pacific, *J. Geophys. Res.*, 77(23), 4432–4460.
- Gagan, M., K. Sieh, W. Hantoro, H. Lynch, R. Edwards, and J. Zachariassen (2000), Coral microatoll seismochemistry and the great Tambora eruption of 1815 AD, paper presented at 9th International Coral Reef Symposium, State Minist. For the Environ., Bali, Indonesia, 23–27 Oct.
- Hsu, Y., M. Simons, J.-P. Avouac, K. Sieh, R. Briggs, A. Meltzner, Y. Bock, C. Subarya, and L. Prawirodirdjo (2005), Coseismic and postseismic slip on the Sumatran megathrust following the 2005 Nias-Simeulue, Indonesia earthquake, *Eos Trans. AGU*, 86(52), Fall Meet. Suppl., Abstract T31C-02.
- Jacoby, G., P. Sheppard, and K. Sieh (1988), Irregular recurrence of large earthquakes along the San Andreas fault in southern California: Evidence from trees near Wrightwood, *Science*, 241, 196–199.
- Kanamori, H. (1973), Mode of strain release associated with major earthquakes in Japan, *Annu. Rev. Earth Planet. Sci.*, 1, 213–239.
- Katili, J. A., and F. Hehuwat (1967), On the occurrence of large transcurrent faults in Sumatra, Indonesia, *J. Geosci.*, 10, 5–17.
- Knutson, D. W., et al. (1972), Coral chronometers: Seasonal growth bands in reef corals, *Science*, 177, 270.
- Krempf, A. (1927), La forme des récifs corallines et le régime des vents alternants, *Mem. Trav. Serv. Oceanogr. Peche Indochine*, 2, 1–3.
- Lay, T., et al. (2005), The great Sumatra-Andaman earthquake of 26 December 2004, *Science*, 308, 1127–1133.
- McCaffrey, R. (1991), Slip vectors and stretching of the Sumatran fore arc, *Geology*, 19, 881–884.
- Melbourne, T. I., F. H. Webb, J. M. Stock, and C. Reigber (2002), Rapid postseismic transients in subduction zones from continuous GPS, *J. Geophys. Res.*, 107(B10), 2241, doi:10.1029/2001JB000555.
- Meriaux, A., K. Sieh, C. Rubin, F. Ryerson, R. Finkel, A. Meltzner, and M. Taylor (2004), Kinematics of the southern Alaska constrained by westward-decreasing post-glacial slip-rates on the Denali fault, Alaska, *Eos Trans. AGU*, 85(47), Fall Meet. Suppl., Abstract G13C-07.
- Nalbant, S., S. Steacy, K. Sieh, D. Natawidjaja, and J. McCloskey (2005), Earthquake risk on the Sunda trench, *Nature*, 435, 756–757.
- Natawidjaja, D. (2003), Neotectonics of the Sumatran Fault and paleogeodesy of the Sumatran subduction zone, Ph.D. thesis, 371 pp, Calif. Inst. of Technol., Pasadena, Calif., 27 Sept.
- Natawidjaja, D. H., K. Sieh, S. N. Ward, H. Cheng, R. L. Edwards, J. Galetzka, and B. W. Suwargadi (2004), Paleogeodetic records of seismic and aseismic subduction from central Sumatran microatolls, Indonesia, *J. Geophys. Res.*, 109, B04306, doi:10.1029/2003JB002398.
- Netscher, E. (1881), Padang in het laatst der XVIIIe eeuw, *Verh. Bataviaasch Genootschap Kunsten Wet.*, 41(7), 122.
- Newcomb, K., and W. McCann (1987), Seismic history and seismotectonics of the Sunda Arc, *J. Geophys. Res.*, 92, 421–439.
- Okada, Y. (1992), Internal deformation due to shear and tensile faults in a half-space, *Bull. Seismol. Soc. Am.*, 82, 1018–1040.
- Prawirodirdjo, L., Y. Bock, and R. McCaffrey (1997), Geodetic observations of interseismic strain segmentation at the Sumatra subduction zone, *Geophys. Res. Lett.*, 24(21), 2601–2604.
- Prawirodirdjo, L., Y. Bock, and J. Genrich (1999), One century of tectonic deformation along the Sumatran Fault from triangulation and GPS surveys, *J. Geophys. Res.*, 105(B12), 28,343–28,361.
- Rivera, L., K. Sieh, and D. Helmberger (2002), A comparative study of the Sumatran subduction-zone earthquakes of 1935 and 1984, *Bull. Seismol. Soc. Am.*, 92(5), 1721–1736.
- Saji, N. H., B. Goswami, P. Vinayachandran, and T. Yamagata (1999), A dipole mode in the tropical Indian ocean, *Nature*, 401, 360–363.
- Savage, J. (1983), A dislocation model of strain accumulation and release at a subduction zone, *J. Geophys. Res.*, 88, 4984–4996.
- Sawai, Y., K. Satake, T. Kamataki, H. Nasu, M. Shishikura, B. Atwater, B. Horton, H. Kelsey, T. Nagumo, and M. Yamaguchi (2004), Transient uplift after a 17th century earthquake along the Kuril subduction zone, *Geophys. Res. Lett.*, 31, 1918–1920.
- Scoffin, T. P., and D. R. Stoddart (1978), The nature and significance of microatolls, *Philos. Trans. R. Soc. London, Ser. B*, 284, 99–122.
- Shen, C.-C., R. Edwards, H. Cheng, J. Dorale, R. Thomas, B. Moran, S. Weinstein, and H. Edmonds (2002), Uranium and thorium isotopic and concentration measurements by magnetic sector inductively coupled plasma mass spectrometry, *Chem. Geol.*, 185(3–4), 165–178.
- Sieh, K. (1984), Lateral offsets and revised dates of large earthquakes at Pallett Creek, California, *J. Geophys. Res.*, 89, 7641–7670.
- Sieh, K. (2005), Aceh-Andaman earthquake: What happened and what's next?, *Nature*, 434, 573.
- Sieh, K., and D. Natawidjaja (2000), Neotectonics of the Sumatran fault, Indonesia, *J. Geophys. Res.*, 105, 28,295–28,326.
- Sieh, K., M. Stuvier, and D. Brillinger (1989), A more precise chronology of earthquakes produced by the San Andreas fault in southern California, *J. Geophys. Res.*, 94, 603–623.
- Sieh, K., S. Ward, D. Natawidjaja, and B. Suwargadi (1999), Crustal deformation at the Sumatran subduction zone revealed by coral rings, *Geophys. Res. Lett.*, 26, 3141–3144.
- Subarya, C., M. Chlieh, L. Prawirodirdjo, J. P. Avouac, Y. Bock, K. Sieh, A. Meltzner, D. Natawidjaja, and R. McCaffrey (2006), Plate-boundary deformation associated with the great Sumatra-Andaman earthquake, *Nature*, 440, 46–51.
- Taylor, F. W., C. Frohlich, J. Lecolle, and M. Strecker (1987), Analysis of partially emerged corals and reef terraces in the central Vanuatu arc: Comparison of contemporary coseismic and nonseismic with Quaternary vertical movements, *J. Geophys. Res.*, 92, 4905–4933.
- Taylor, F. W., R. Edwards, and G. Wasserburg (1990), Seismic recurrence intervals and timing of aseismic subduction inferred from emerged corals and reefs of the central Vanuatu (New Hebrides) frontal arc, *J. Geophys. Res.*, 95, 393–408.
- Thatcher, W., and J. Rundle (1984), A viscoelastic coupling model for the cyclic deformation due to periodically repeated earthquakes at subduction zones, *J. Geophys. Res.*, 89, 7631–7640.
- Vigny, C., A. Socquet, C. Rangin, N. Chamot-Rooke, M. Pubellier, M. Bouin, G. Bertrand, and M. Becker (2003), Present-day crustal deformation around Sagaing fault, Myanmar, *J. Geophys. Res.*, 108(B11), 2533, doi:10.1029/2002JB001999.
- Ward, S. (2001), Landslide tsunami, *J. Geophys. Res.*, 106, 11,201–11,215.
- Weldon, R., K. Scharer, T. Fumal, and G. Biasi (2004), Wrightwood and the earthquake cycle: What a long recurrence record tells us about how faults work, *GSA Today*, 14, 4–10.
- Wichmann, A. (1918), Die Erdbeben des Indischen Archipels bis zum Jahre 1857. Verhandlungen der Koninklijke Akademie van Wetenschappen te Amsterdam (Tweede Sectie), *Deel XX 4*, Johannes Müller, Amsterdam.
- Yalciner, A., P. Perincek, S. Ersoy, G. Presateya, R. Hidayat, and B. McAdoo (2005), December 26, 2004 Indian Ocean Tsunami Field Survey (Jan. 21–31, 2005) at North of Sumatra Island, report, UNESCO IOC, Paris.
- Zachariassen, J. (1998), Paleoseismology and paleogeodesy of the Sumatran Subduction Zone: A study of vertical deformation using coral microatolls, Ph.D. thesis, 418 pp, Calif. Inst. of Technol., Pasadena, 3 Oct.
- Zachariassen, J., K. Sieh, F. Taylor, R. Edwards, and W. Hantoro (1999), Submergence and uplift associated with the giant 1833 Sumatran subduc-

tion earthquake: Evidence from coral microatolls, *J. Geophys. Res.*, *104*, 895–919.

Zachariasen, J., K. Sieh, F. Taylor, and W. Hantoro (2000), Modern vertical deformation at the Sumatran subduction zone: Paleogeodetic insights from coral microatolls, *Bull. Seismol. Soc. Am.*, *90*, 897–913.

J.-P. Avouac, K. Sieh, M. Chlieh, and J. Galetzka, Tectonics Observatory, California Institute of Technology 100-23, Pasadena, CA 91125, USA. (sieh@gps.caltech.edu)

H. Cheng and R. L. Edwards, Department of Geology and Geophysics, University of Minnesota, 310 Pillsbury Drive Southeast, Minneapolis, MN 55455, USA.

D. H. Natawidjaja and B. W. Suwargadi, Puslit Geoteknologi, Komplek LIPI Gd.70, Jl. Sangkuriang, Bandung 40135, West Java, Indonesia.

S. N. Ward, Institute of Geophysics and Planetary Physics, University of California, Santa Cruz, CA 95064, USA.